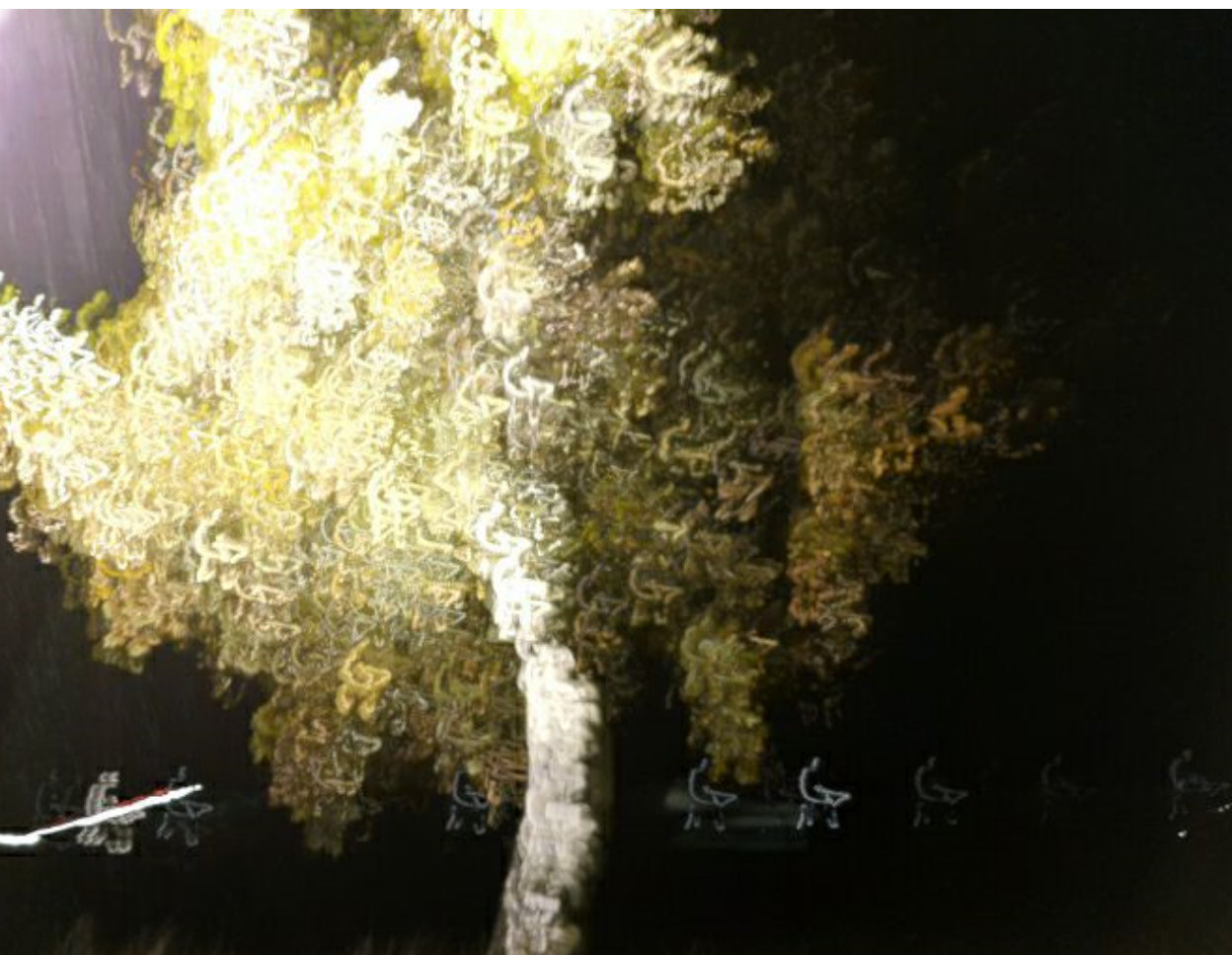# Fractionation of woody biomass

lignin and suberin in focus

Ivan Kumaniaev

Fractionation of woody biomass
lignin and suberin in focus

Ivan Kumaniaev

Academic dissertation for the Degree of Doctor of Philosophy in Organic Chemistry at Stockholm University to be publicly defended on Friday 4 December 2020 at 10.00 in Magnélisalen, Kemiska övningslaboratoriet, Svante Arrhenius väg 16 B.

Abstract

This thesis is dedicated to the research of fractionation and valorization of different types of woody biomass. In the first part, oak (*Quercus suber*) and birch (*Betula pendula*) barks are considered. Bark is the outer layer of wood and is treated as waste in the current wood processing technologies. The main polymers which form bark are lignin (aromatic polyether) and suberin (aliphatic polyester). In the present study, these compounds have been transformed into monomeric phenols which may serve as a precursors for bio-based polyesters, and hydrocarbon bio-oil of gasoline, diesel, and heavy gas oil ranges. The bio-oil has been studied with GC-MS, 2D GC, and simulated distillation techniques.

The second part concerns birch heartwood. In contrast with bark, wood does not contain suberin but has a higher content of lignin. A variety of fractionation processes are known for wood. The major disadvantages are contamination of pulp with catalyst and irreversible recondensation of lignin which takes place in harsh pulping conditions. For the purpose of solving these problems, a flow process has been developed in which the biomass and the catalyst are separated in time and space and the lignin is stabilized and cleaved into monomers immediately after its extraction. The process has been optimized to obtain monophenolic lignin-derived compounds, while the remaining cellulose pulp was enzymatically converted into glucose. Hemicellulose serves as a hydrogen donor for the lignin reduction, and therefore no external hydrogen source is required. The experimental work was complemented with a theoretical study of the process of lignin cleavage on the Pd surface. Computations under on the ReaxFF approach were used to model the successive steps of the adsorption of the molecules on the catalyst, their fragmentation, reactions, and desorption. The products obtained in the experiment have been also observed in this simulation.

Keywords: *lignocellulose, lignin, suberin, biomass, palladium, catalysis, flow chemistry.*

Department of Organic Chemistry

Stockholm University, 106 91 Stockholm

FRACTIONATION OF WOODY BIOMASS

Ivan Kumaniaev

Fractionation of woody biomass

lignin and suberin in focus

Ivan Kumaniaev

Грустно думать, что напрасно
была нам молодость дана.

А.С.Пушкин

Abstract

This thesis is dedicated to the research of fractionation and valorization of different types of woody biomass. In the first part, oak (*Quercus suber*) and birch (*Betula pendula*) barks are considered. Bark is the outer layer of wood and is treated as waste in the current wood processing technologies. The main polymers which form bark are lignin (aromatic polyether) and suberin (aliphatic polyester). In the present study, these compounds have been transformed into monomeric phenols which may serve as a precursors for bio-based polyesters, and hydrocarbon bio-oil of gasoline, diesel, and heavy gas oil ranges. The bio-oil has been studied with GC-MS, 2D GC, and simulated distillation techniques.

The second part concerns birch heartwood. In contrast with bark, wood does not contain suberin but has a higher content of lignin. A variety of fractionation processes are known for wood. The major disadvantages are contamination of pulp with catalyst and irreversible recondensation of lignin which takes place in harsh pulping conditions. For the purpose of solving these problems, a flow process has been developed in which the biomass and the catalyst are separated in time and space and the lignin is stabilized and cleaved into monomers immediately after its extraction. The process has been optimized to obtain monophenolic lignin-derived compounds, while the remaining cellulose pulp was enzymatically converted into glucose. Hemicellulose serves as a hydrogen donor for the lignin reduction, and therefore no external hydrogen source is required. The experimental work was complemented with a theoretical study of the process of lignin cleavage on the Pd surface. Computations under the ReaxFF approach were used to model the successive steps of the adsorption of the molecules on the catalyst, their fragmentation, reactions, and desorption. The products obtained in the experiment have been also observed in this simulation.

Populärvetenskaplig sammanfattning

För närvarande produceras huvuddelen av bränslen och material från fossila källor. Fastän denna råvara är billig, finns i rikligt, mängd samt har varit en viktig resurs för vårt välstånd, så har decenniers användning lett till växthusutsläpp som orsakar klimatförändringar. Av den anledning letar forskare efter andra resurser som på sikt skulle vara mer pålitliga och miljövänliga. Exempel är sol- och vindkraftverk som används för fossilfri produktion av energi. Tyvärr kan inte dessa källor möta våra behov vid tillverkning av mediciner, material och vissa behov inom transporter. Därför behöver vi alternativ till råoljan och en kandidat är växtbiomassa, vilket är av särskilt intresse för sådana länder som Sverige, det vill säga de länder som är rika på skogens resurser.

I den här avhandlingen ägnar vi oss åt omvandling av olika träslag till bränslen och kemikalier. I kapitel 2 och 3 beskrivs vårt arbete med trädbark som är en avfallsprodukt från skogsindustrin. Bark upplösas och omvandlas till kolväten för användning som biobränsle. I kapitel 4 och 5 utvecklas en reaktorteknik för separering av olika komponenter i björkträ. De erhållna produkterna kan användas som reagens för att tillverka hållbara polymerer som potentiellt kan ersätta fossila plaster.

Vi hoppas att detta arbete kommer att bidra till utvecklingen mot en fossilfri ekonomi i Sverige.

List of publications

The thesis is based on the following papers:

I. Valorization of *Quercus suber* bark toward hydrocarbon bio-oil and 4-ethylguaiacol
Ivan Kumaniaev and Joseph S. M. Samec
ACS Sus. Chem. Eng., **2018**, *6*, 5737–5742

II. Conversion of birch bark to biofuels
Ivan Kumaniaev, Kranti Navare, Natalia Crespo Mendes, Vincent Placet, Karel Van Acker and Joseph S. M. Samec
Green Chem., **2020**, *22*, 2255–2263

III. Lignin depolymerization to monophenolic compounds in a flow-through system
Ivan Kumaniaev, Elena Subbotina, Jonas Sävmarker, Mats Larhed, Maxim V. Galkin and Joseph S. M. Samec
Green Chem., **2017**, *19*, 5767–5771

IV. ReaxFF Simulations of Lignin Fragmentation on a Palladium-Based Heterogeneous Catalyst in Methanol–Water Solution
Susanna Monti, Pemikar Srifa, Ivan Kumaniaev and Joseph S. M. Samec
J. Phys. Chem. Lett., **2018**, *9*, 5233–5239

V. Adsorption Isotherms of Lignin-Derived Compounds on a Palladium Catalyst
Ivan Kumaniaev and Joseph S. M. Samec
Ind. Eng. Chem. Res., **2019**.

Contribution report

I. Performed all experimental work except 2D GC and simulated distillation, wrote the manuscript and the supporting information.

II. Performed all experimental work except 2D GC and simulated distillation, participated in writing of the manuscript and the supporting information. Participated in the theoretical evaluation of energy efficiency of the process.

III. Performed experimental work: flow reactions, analysis of biomass, synthesis of model compounds. Wrote the supporting information. Participated in the writing of manuscript.

IV. Contributed to the design of the project based on experiments in paper III, discussions regarding interpretation of results of computation, and the preparation of the manuscript.

V. Performed experimental work, wrote the manuscript and the supporting information.

Publications not included in this thesis

VI. A combination of experimental and computational methods to study the reactions during a Lignin-First approach
Ivan Kumaniaev, Elena Subbotina, Maxim V. Galkin, Pemikar Srifa, Susanna Monti, Isara Mongkolpichayarak, Duangamol Nuntasri Tungasmita and Joseph S. M. Samec
Pure and Applied Chemistry, **2020**.

Contents

1. Introduction

1.1. Woody biomass

Biomass is a collective term for organic matter derived from biological sources (e.g. plants or animals).[1] The most available type of biomass is ligno-cellulose, obtained from higher plants. Its main components are lignin (15–35%), cellulose (38–50%), and hemicellulose (23–32%), bound to each other to form lignin-carbohydrate complexes (LCC).[2] In the case of bark, the list of components is amplified with suberin (20–40%).[3] Apart from the polymeric components, biomass also contains a variety of weakly bonded compounds of low molecular weight, such as alkanols, carboxylic acids, terpenes and betulin, which usually can be removed by extraction (up to 40% in bark).[4] In this thesis, bark is distinguished from internal tissues present in trees (heartwood, sapwood etc.) which are referred to as "wood".

1.1.1. Lignin

Lignin (Figure 1) is an aromatic polyether of a complex branched structure. It is synthesized in plant tissues in the process of radical oxidative coupling of hydroxycynnamyl alcohols, namely, coniferyl, sinapyl and coumaryl.[5] The monomers form different types of bonds but the most abundant one is β-O-4' (ca. 70% of all linkages). The starting point of the polymerization mechanism is an enzymatically catalyzed radical oxidation of monolignols with hydrogen peroxide,[6] leading to the formation of resonance-stabilized phenoxide radicals.[7] The radicals then undergo coupling reactions (Scheme 1).

The lignin content in biomass heavily depends on its source and also on the part of a plant which it has been derived from. Hardwood (birch, maple, poplar, eucalyptus) contains 18 to 25 wt.% of lignin, while for softwood (spruce, pine) this value is 25 to 35 wt.%, and for grasses 10 to 30 wt.%.[8] The tree parts which possess the highest lignin content are the external ones such as bark. On the contrary, leaves contain no lignin but instead contain large amounts of hemicellulose (85%).[9]

The types of lignin monomers also vary and depend on the plant type. Hardwood lignin is predominantly composed of syringyl, softwood lignin of guaiacyl, and grass lignin of coumaryl units.[10]
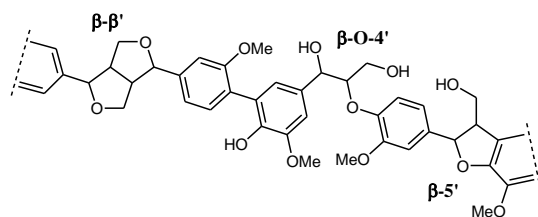
Figure 1. A simulative fragment of lignin structure. The dominant types of linkages are depicted.
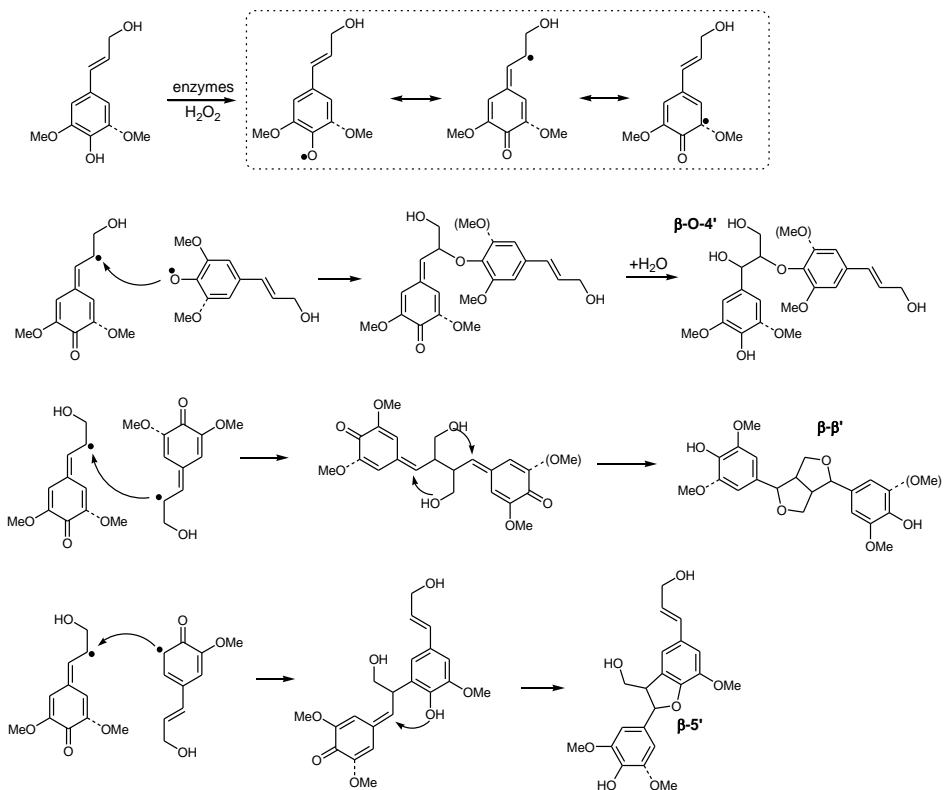
Scheme 1. Pathways of formation of different types of interunit linkages in lignin.

1.1.2. Suberin

Suberin (Figure 2) is found in external and growing tissues of plants and plays the role of protective barrier.[11] In contrast with lignin, suberin is an aliphatic polyester, presumably comprising mono- and polyhydroxylated fatty acids, though minor amounts of typical monolignol derivatives are also present. The monomers are bound through ester linkages.[12,13]

The suberized tissues possess a lower oxygen content than wood. For instance, the O:C ratio of *Quercus suber* bark, used in our studies was measured to be 0.46, which is significantly lower than for wood (0.6−0.7).[14] Therefore, suberin may be considered to have a good potential as a biofuel precursor due to its low oxygen content.
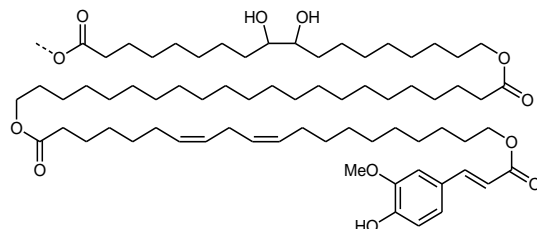
Figure 2. A simulative fragment of suberin structure. Both aliphatic and aromatic types of monomers are shown.

1.1.3. Carbohydrates

The two major types of carbohydrates present in higher plants are cellulose and hemicellulose (Figure 3). Both are of polymeric nature. Cellulose consists of glucose monomers linked with β-1,4-bonds; the amount of monomers varies from hundreds to thousands per each chain. During the process of biosynthesis, the growing cellulose polymers are assembled into microfibrills stabilized with non-covalent interactions such as van der Waals and hydrogen bonds. The microfibrills are in their turn packed into fibers, and thus the whole structure becomes crystalline-like and insoluble, though it contains both well-ordered and amorphous domains.

The term 'hemicellulose' refers to a heterogeneous group of polysaccharides such as mannans, xylans, and galactans. They are composed of partially acetylated pentoses and hexoses linked through 1,3, 1,6, and 1,4-glycosidic bonds. The resulting polymeric structures are more branched, labile, and amorphous than the structure of cellulose and act as links between cellulose and lignin. Hemicellulose is much more prone to degradation and depolymerization than cellulose and thus is readily removed upon biomass treatment.

Figure 3. Simulative fragments of structures of cellulose (**a**) and hemicellulose (**b**).

1.2. Valorization of the biomass

Biomass is a renewable matter as it is continuously formed in the biosphere. Together with a high energy content, this property is the reason why different pathways of biomass transformation towar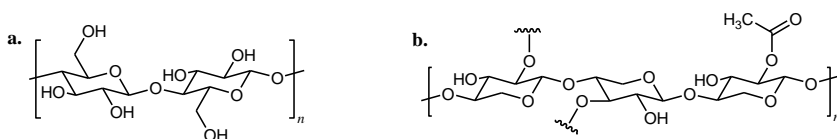d fuels and chemicals are being widely explored. Such technologies would make it possible to liquidate the dependence on fossil oils.[15,16,17] In general, biomass can be valorized in a number of ways, in accordance with the composition of each feedstock. It may be converted into syngas or bio-oil by gasification, pyrolysis and liquefaction processes, and also converted into value-added compounds and platform chemicals.

In order to perform further transformations efficiently, it is necessary to separate lignin and other hydrophobic components from the hydrophilic carbohydrate domain, i.e. to fractionate the biomass.[18] Several industrially used methods have been developed, such as sulfite, kraft, soda, and organosolv pulping processes.[19] In these processes, lignin is solubilized and thus cellulosic fibers are made free of the lignocellulosic matrix, i.e. pulp is obtained. The separation becomes possible due to partial depolymerization of lignin and the breakdown of lignin-carbohydrate complexes. Therefore, the pulping procedures lead to significant modification of the structure of the separated lignin.[20]

A variety of well-established processes are developed for the valorization of the carbohydrate part of the biomass for production of paper, nitrocellulose and cellulose fibers, as well as monomeric sugars (glucose) and valuable chemicals: xylitol, furfural, 5-hydroxymethylfurfural, γ-valerolactone, and organic acids.[21,22,23] Processes of valorization of suberin and lignin domains are less developed. This thesis focuses on the treatment of lignin and suberin domains.

1.2.1. Traditional pulping methodologies

The main pulping methodology currently used in industry is the kraft pulping which accounts for about 85% of world lignin generation ($4 \cdot 10^7$ tons per year).[24] The procedure involves treatment of the biomass with an aqueous alkaline/sulfide solution (typically, Na_2S and $NaOH$) at 160–180 °C for several hours. During the process, lignin and hemicellulose are partially degraded, depolymerized, and solubilized while cellulose remains as a solid in the form of pulp. Acidification of the resulting solution (black liquor) makes it possible to isolate the lignin precipitate.[25] The remaining liquid is then treated in a boiler in order to recycle inorganic chemicals.

The kraft lignin thus obtained has an average molecular weight of 1000–3000 Da (with maximum of $1.5 \cdot 10^4$ Da and polydispersity index PD = 2.5–3.5).[26] This product is significantly modified as compared to the native lignin. Strongly alkaline conditions lead to the formation of quinone methide intermediates (Scheme 2) which then undergo polycondensation reactions by

means of the formation of new C–C bonds, inclusion of sulfur-containing groups into the polymer structure and the increase of the average molecular weight. In particular, the abundance of β-O-4' bonds is significantly lowered.[27] The new polycondensated structures are not prone to cleavage and catalytic transformations because C–C bonds have high dissociation energies and the sulfur-containing groups are poisonous to the metal catalysts.[28] Also, the lignin is contaminated with the products of hemicellulose decomposition and fatty acids. Therefore, further valorization of the kraft lignin is complicated.

Another important type of industrial pulping is the process in which biomass is treated with an aqueous sulfite at 120–150° C (sulfite pulping).[29] The general methodology is the same: lignin is dissolved while cellulose remains solid. Production of lignosulfonates (10^6 ton per year) is lower than the production of kraft lignin.[30] An advantage of this method is the lower degree of degradation of the obtained lignin as compared to the kraft one; also, some polar groups in the lignin structure are generated which favor its higher solubility. However the β-O-4' are as well labile under the pulping conditions and their cleavage results in the formation of sulfonated oligolignols. Molecular weight of the generated lignosulfonates significantly varies (1000 to $5 \cdot 10^4$ Da, PD = 4.2–7.0). The main contaminants are carbohydrates and ash. Lignosulfonates are used in different fields of industry, such as production of vanillin, surfactants, and dispersing agents.[31]
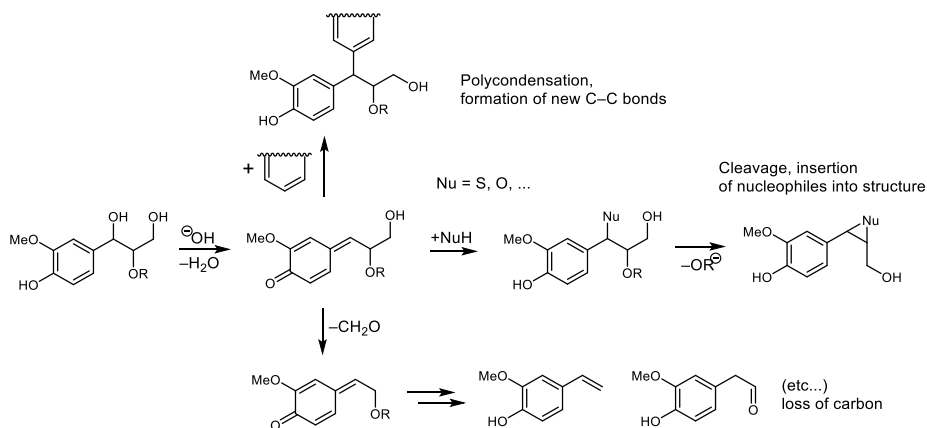
Scheme 2. Overview of lignin transformations taking place upon pulping of woody biomass.

1.2.2. Organosolv pulping

Organosolv methodology has been developed with an intention to provide a more environmentally-friendly pulping technique.[32] In this type of process, the biomass is treated with organic solvents (MeOH, EtOH, dioxane) mixed with water in the presence of acids and other additives (such as peroxides) at 180–200°C.[33] The bonds between lignin and carbohydrates are broken and the lignin is released in a form which is relatively close to the native one. This affords to implement further valorization procedures. The major side reaction is the acid-catalyzed formation of benzylic cations due to water subtraction from α positions of the β-O-4' bonds; these intermediates then undergo condensation reactions with electron-rich aromatic rings. Despite this, average molecular weight of the **extracted** lignin is 500 to 5000 Da (PD ~ 1.5) which is lower than in case of traditional pulping methods.[33] The major drawback of the methodology is low quality of the obtained cellulose fibers. This is the reason why organosolv pulping is not widely used in industry.
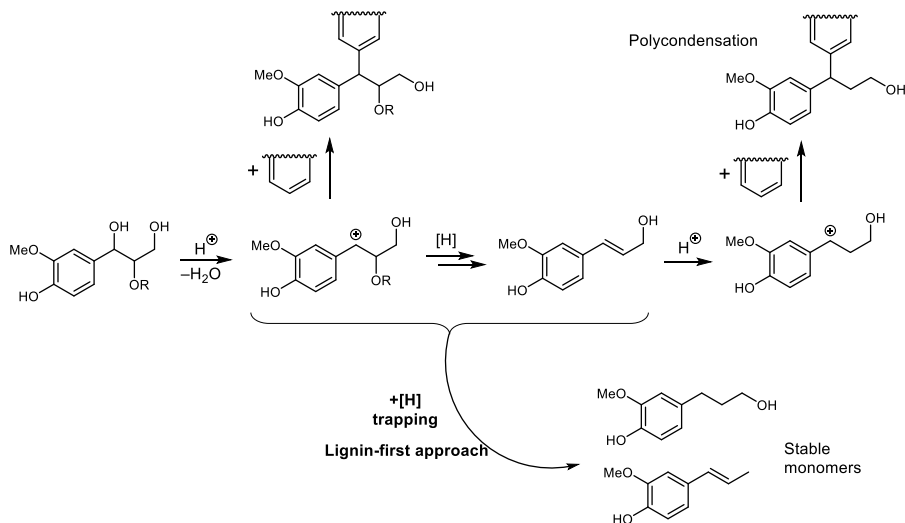
1.2.3. Lignin-first approach

In the typical organosolv pulping conditions, the extracted lignin still undergoes recondensation processes which lead to the formation of new C–C bonds (Scheme 3). This causes an increase of the molecular weight of lignin, tangles its structure and makes isolation of products and further valorization difficult. In order to overcome these issues, a number of so-called lignin-first approaches was investigated, focusing on even more effective lignin preservation and isolation. Other terms used in the literature include "Catalytic biomass fractionation" and "Catalytic upgrading biorefinery". These approaches also facilitate valorization of other biomass components, which are carbohydrates.[34]

In this type of processes, biomass is subjected to modified organosolv pulping procedure. The extracted lignin undergoes *in situ* catalytic transformations and forms stable products, i.e. intermediates are directly trapped and prevented from recondensation. The cellulose remains intact in the form of solid pulp. Other carbohydrates (hemicellulose) are either preserved, extracted together with lignin or utilized as the hydrogen source in the lignin transformation. Polar products may be separated by extraction with water.

The groups of Rinaldi,[35] Sels,[36] Abu-Omar,[37] Kou,[38] and our own,[39] showed that the promising type of lignin-first approach involves the reduction of the generated lignin monomers as the trapping reaction. One of the recent articles reports a simple type of lignin-first approach in which organosolv lignin is trapped and stabilized using protection of 1,3-diol moiety of β-O-4' linkages with formaldehyde.[40]

As well as other pulping methodologies, processes based on lignin-first approach have so far been performed in batch reactors by mixing together bi-

omass and the catalyst. As a result, purification of the pulp becomes compli-
cated. Moreover, in such a system it is difficult to investigate the reaction
mechanisms involved, i.e. the individual roles of the solvent mediated solvol-
ysis and the catalyst promoted depolymerization and also the nature of inter-
mediates.

Scheme 3. Polycondensation problem arising in the organosolv pulping
processes and how lignin-first approach allows to avoid it

1.2.4. Suberin isolation, characterization, and valorization

The general requirement for suberin depolymerization is to apply alkaline
conditions which promote the cleavage of ester bonds. This is in conflict with
the goal to depolymerize lignin smoothly which demands implementation of
acidic medium.[41]

The typical analytical procedure for suberin isolation involves refluxing of
the biomass sample with 1–5% solution of sodium methoxide in methanol. In
these conditions, suberin undergoes methanolysis (Scheme 4) and is removed.
Lignin and carbohydrates remain relatively intact. Afterwards, the solution is
diluted with water and suberin derivatives are extracted with organic solvent
such as chloroform, dichloromethane, or ether. The organic fraction may then
be subjected to GC-MS or NMR analysis. A number of variations of this pro-
cedure have been studied, including steam explosion and enzymatic pretreat-
ments of the biomass. Methanolysis enables to extract suberin completely with
typical yields of 20–40% of bark weight. [13]

One of the reported fractionation procedures which allows to isolate su-
berin implements typical lignin-first approach conditions. In the procedure,
suberin is partially depolymerized into a range of fatty acids and alcohols.

Further depolymerization in alkaline conditions is needed to accomplish the transformation.[42] Another method involves FeCl3-catalyzed lignin isolation; however, the suberin part was not described in detail in the original paper.[43]
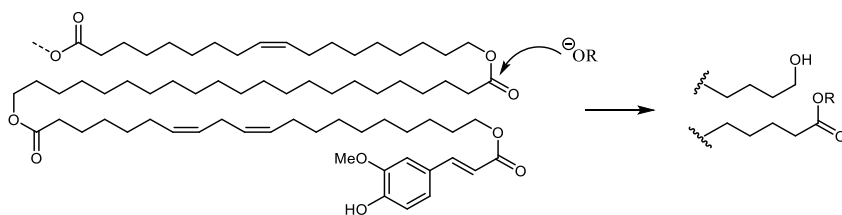
Scheme 4. Depolymerization of suberin through methanolysis of ester bonds.

1.2.5. Further transformation of suberin and lignin into chemicals and fuels

Transformation of the lignin and suberin into a biofuel requires a further deoxygenation. However, the oxygen content in lignin is rather high (25–30%). This is the reason why development of lignin-based biofuels remains a challenge,[44] though a variety of deoxygenative processes was developed leading to alkanes and alkanols. Another issue is the complexity of structures of lignins obtained in common pulping processes.

Products of partial lignin deoxygenation and depolymerization may also be of interest. The lignin structure itself involves a range of motifs which can serve as building blocks for valuable chemicals such as pharmaceuticals and polymers (Scheme 5)[45]. Therefore, full removal of oxygen and defunctionalization may be a less rational approach than utilization of the present fragments. As shown recently, it is possible to use phenols obtained from lignin as precursors for green polymers.[44]
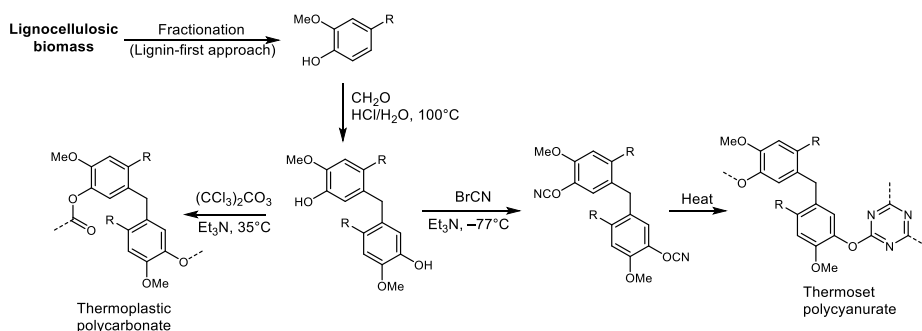
Scheme 5. Lignin-derived precursors for polymers.[44]

Structures of suberin and the products of its depolymerization are simpler, possess lower oxygen content (15–20%) and therefore it is easier to convert suberin into fuel-type compounds. However, to our knowledge, procedures for

full suberin deoxygenation have not been previously developed. One of our intentions was to fill this gap.

The basis for such a procedure should be found among the variety of already known methods of the deoxygenation of carboxylic acids and alcohols. Catalytic deoxygenation of fatty acids in the gas phase was demonstrated in 1982,[46] with decarboxylation of octanoic acid over palladium and nickel.[47] Hydrocracking of fatty acids and triglycerides toward C_{15}–C_{21} hydrocarbons was shown to be catalyzed by NiO-MoO_3 and CoO-MoO_3 bimetallic systems at 350–450 °C and 48–150 bar.[48] Similar reactions have also been shown to proceed over activated Al_2O_3.[49,50] The side products are ketones formed as the result of condensation of two molecules of a carboxylic acid.[49]

Subsequently, liquid phase reactions were explored using several types of catalysts of different nature. Both hydrogenation as well as subtraction of carboxylic group was studied extensively using stearic acid as a model compound,[51] implementing a wide scope of metal catalysts (Pd, Pt, Mo, Ni, Ru, Rh, Ir, and Os, as well as oxide-based and bimetallic catalysts). Several supports were explored such as zeolites, activated carbon and mesoporous synthetic carbon, as well as oxides (Cr_2O_3, SiO_2, Al_2O_3). Pd and Pt on carbon were found to be the most promising catalysts for this type of reaction. Complete decarboxylation of stearic acid into heptadecane was achieved over palladium on microporous carbon at 300 °C and 6 hours reaction time.

An efficient bimetallic Pt-MoO_x catalysts with a TiO_2 support for the conversion of various biomass-related oxygenated compounds have recently been reported.[52] The catalyst afforded higher turnover numbers than previously described ones. The process is solvent-free and provides alkanes as products. The important feature is that the reaction proceeds without C–C bond cleavage, i.e. there is no carbon atom loss.

The mechanism of the reaction in connection with the catalyst structure have been investigated. Kinetic curves of concentrations of intermediates and side products supported the idea of stepwise reduction of carboxylic group (Scheme 6, a). IR study of the ketone absorption led to the conclusion that the catalyst activity emerges due to cooperation between Pt atoms and the Lewis acid sites of MoO_x (Scheme 6, b). The C=O stretching band was shifted from 1703–1709 cm^{-1} (observed over other Pt catalysts) to 1690 cm^{-1} (over Pt-MoO_x/TiO_2). This suggests that the C=O bond was weakened by the coordination to Mo^{n+} acidic sites.

Thus, the deoxygenation of the biomass-derived compounds is well developed and it would be easy to apply the modified procedures to the new feedstock such as bark.
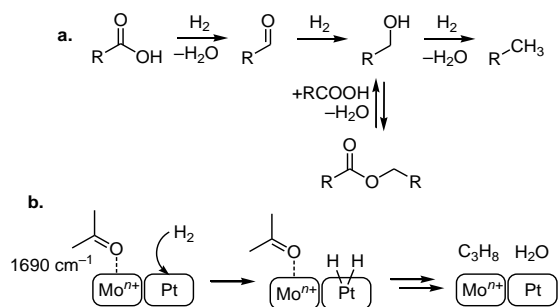
Scheme 6. Steps of the carboxylic group reduction over Pt-MoO$_x$/TiO$_2$ (**a**), the cooperation of Pt and Mo^{n+} catalytic sites (**b**).

1.3. Aim of the thesis

This thesis focuses on the study and development of methods for valorization of two types of biomass: wood and bark. The general strategy is catalytic reductive depolymerization of lignin (in case of wood) and both lignin and suberin (in case of bark) using environmentally-friendly procedures.

Specific goals include:

• investigate whether a lignin-first approach can be applied to bark to both depolymerize the suberin and lignin.

• study the product composition resulting from lignin first methodology applied to bark.

• evaluate the possibility of further valorization of the product composition from bark.

• elucidate whether flow-through conditions can be applied to the lignin-first approach, i.e. if pulping and the catalytic stages can be separated in space and time.

• establish the individual roles of pulping and the catalysis in the lignin-first process on wood.

2. Valorization of oak bark toward hydrocarbon bio-oil and 4-ethylguaiacol (paper I)

2.1. Background

Bark is the external protective layer of plants' stems. In the current biomass processing technologies, the bark is usually separated from wood and treated as waste, i.e. burnt to produce heat and electricity.[42]
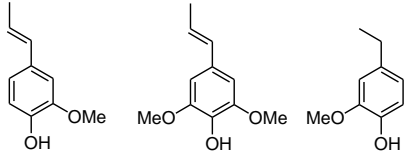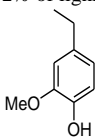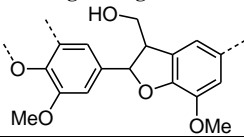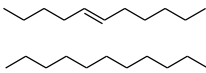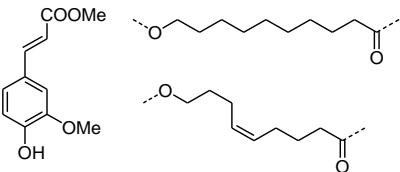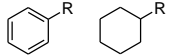
The chemical composition of bark includes weakly bonded extractives (mainly glycerides, 10–40 wt.%), suberin (20–40%), lignin (10–20%), and polysaccharides (10–30%).[53] Bark therefore includes larger amounts of components with high energy content when compared to wood in which carbohydrates are prevalent. As a result, bark exhibits higher energy content: typical heat of bark combustion[14] is 24 MJ·kg^{-1} while for wood this value is 21 MJ·kg^{-1}. This supports the idea to convert bark into fuel-type compounds. Furthermore, the oxygen of bark can be easily removed using a variety of previously developed procedures of hydrodeoxygenation of carboxylic acids, esters, and alcohols.[45]

In this work, we investigate whether the lignin-first approach can be applied to *Quercus suber* which is used as a model of bark such as birch bark and develop a process which would afford parallel transformation of both lignin and suberin, and investigate if the bark may act as a source of valuable chemicals and fuel-range hydrocarbons.

2.2. The process overview

A procedure including three steps was envisioned (Table 1). 1) Organosolv pulping is performed in the presence of Pd/C catalyst. Lignin and suberin are partially depolymerized and also lignin is reduced. 2) Volatile monomeric derivatives of lignin are separated by distillation in vacuum. 3) The residue is subjected to hydrodeoxygenation, affording a range of hydrocarbons.

Table 1. Overview of the developed process of bark valorization.

Feedstock	Stage 1	Stage 2
***Quercus suber* bark** 31% suberin 21% lignin 12% carbohydrates 12% extractives 5% moisture	**Monomeric derivatives of lignin** 	**4-ethylguiacol** 2.6% of bark, 12% of lignin
	Lignin oligomers 	**Various hydrocarbons** Average composition $C_{14.9}H_{28.4}O_{0.00-0.06}$ 42% of bark 77% of suberin+lignin 64% of total bark carbon
	Partially hydrolyzed suberin and extractives 	

2.3. Organosolv pulping of bark

The main challenge is to accomplish transformation of both lignin and suberin at the same time. This means that both ether and ester linkages should be cleaved. These two processes are known to be favored at different pH values. Lignin depolymerization proceeds more fluently in acidic or neutral conditions in which suberin is not hydrolyzed. On the other hand, alkaline conditions facilitate suberin hydrolysis but also lead to the processes of lignin recondensation, thus decreasing the yield of lignin monomers. The dependence of yields of different lignin products on the medium pH has been studied in detail.[40] The challenge of suberin depolymerization in neutral media is also mentioned in the literature[41] and is confirmed by our studies.

As a starting point, we considered a method of tandem organosolv pulping with palladium-catalyzed hydrogenolysis which, for heartwood, has been developed in our group previously. The bark was subjected to organosolv pulping in MeOH–H_2O mixture at 200 °C in the presence of 5% Pd/C catalyst. Optionally, acidic or basic additives were used.

Under the employed reaction conditions, the lignin is extracted and reductively cleaved into monomers and oligomers. It was previously shown that carbohydrates present in the biomass, formates derived in situ during pulping, or solvent (methanol) may all serve as the sources of hydrogen equivalents which are transferred to lignin by the Pd/C catalyst.[38,40,54] Therefore this step of the developed process does not require any external hydrogen source. In

parallel with lignin cleavage, methanolysis of suberin takes place, and the formed oligomeric esters are also extracted into the pulping solution.

We performed a brief optimization of the reaction conditions with respect to the goal of transforming both lignin and suberin. GC-MS was used for monitoring of composition of the obtained mixture of monomers. First, we performed the reaction in typical organosolv conditions, either neutral or acidic ones (2.8 g·L^{-1} H$_3$PO$_4$ in MeOH–H$_2$O 2:1 v/v, Figure 4, A, B). This type of solvent system is efficient for wood fractionation, as shown in paper III (Chapter 4). Indeed lignin monomers (**1–8**) were observed, however suberin remained intact (no fatty acid derivatives were observed).
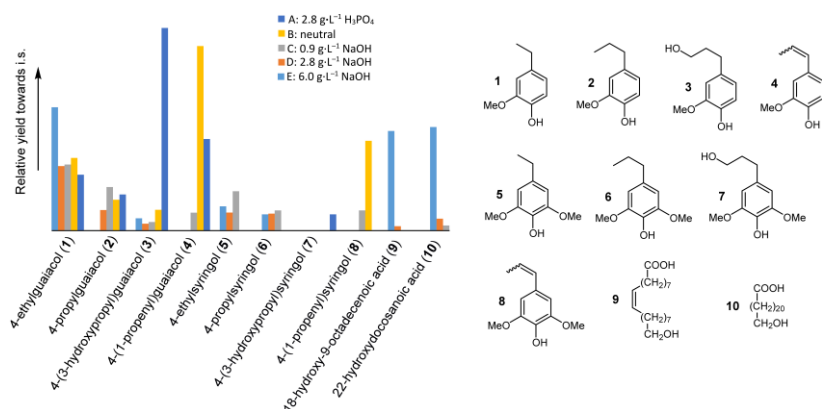
Figure 4. Products of the first step of the process: organosolv pulping combined with transfer hydrogenolysis.

Then we examined the reaction in the alkaline conditions (0.9 to 6.0 g·L^{-1} NaOH, Figure 11, C, D, E) in order to facilitate the suberin cleavage. The yield of fatty acids gradually increased as the base concentration raised and the yield of lignin monomers decreased, as expected. However, for two reasons we decided to continue using the alkaline medium (6.0 g·L^{-1} NaOH). First, the alkaline conditions enabled us to perform both transfer hydrogenolysis of lignin and alkaline methanolysis of suberin in parallel in one step. Second, even though the overall yield of identified lignin derivatives is lower than in case of neutral and acidic conditions, the selectivity of the reaction is higher: 4-ethylguaiacol (**1**) of 90% purity (according to NMR and GC data) can be separated. Meanwhile, selectivity of the reaction in neutral and acidic media is about 50% toward the main product (4-(3-hydroxypropyl)guaiacol (**3**) or 4-propenylguaiacol (**4**)).

The structure of 4-ethylguaiacol (**1**) differs from the structures of products obtained in the neutral and acidic media (**2, 3, 4, 6, 7, 8**) by means of the alkyl chain length (ethyl instead of propyl or propenyl). Shortening of the side chain of monolignolic derivatives in alkaline conditions is a well-known process. It most likely proceeds through a quinone methide intermediate losing a formal-

dehyde molecule.[40] Another possible precursor of 4-ethylguaiacol (**1**) is ferullic acid, one of the minor suberin monomers. A model study showed that under the employed reaction conditions (in the presence of Pd/C and alkali) ferullic acid undergoes decarboxylation and thus generates 4-ethylguaiacol (**1**).

The main products of suberin cleavage observed in the reaction mixture (Figure 5) were 18-hydroxy-9-octadecenoic acid (**9**) and 22-hydroxydocosanoic acid (**10**). Other suberin monomers detected by the analysis of the bark feedstock, such as 20-hydroxyeicosanoic acid and 24-hydroxytetracosanoic acid, were not found. Therefore, suberin depolymerization is not complete and the products entering the next step of the valorization process are of oligomeric nature. This conclusion was confirmed with a kinetic study of the deoxygenation step.
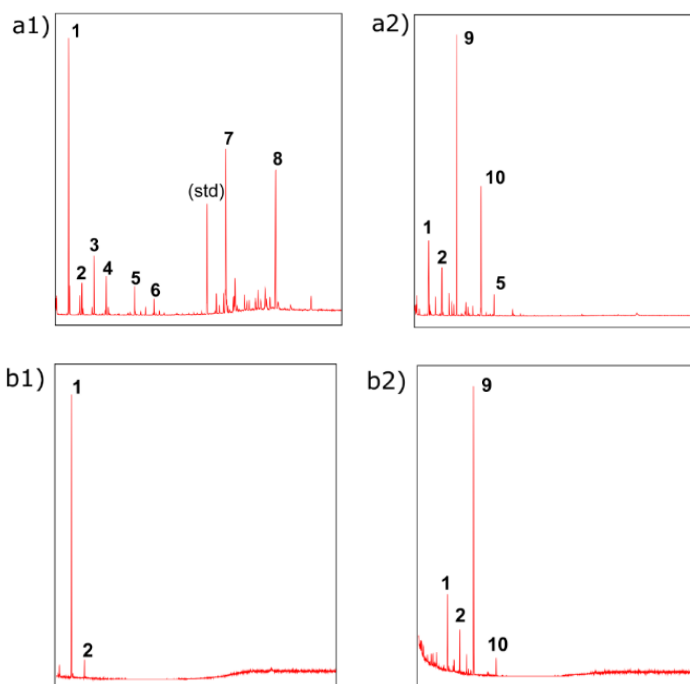

Figure 5. Gas chromatograms of products obtained at different steps of the process (in the form of TMS derivatives). Step 1 (a): Partial depolymerization and formation of monomeric phenols; alkaline media (a1) and neutral media (a2). Step 2 (b): Monomeric phenolic com-pounds obtained in alkaline media (b1) and neutral media (b2), separat-ed by distillation.

2.4. Isolation of 4-ethylguaiacol

4-Ethylguaiacol (**1**) was separated by means of simple vacuum distillation using Kugelrohr (150 °C, 1 mbar). The product of 90% purity (NMR, GC-MS) was obtained as a colorless liquid. The yield corresponds to 12% with respect to the initial content of acid insoluble lignin initially present in the bark feedstock. The major contaminants were guaiacol and 4-propylguaiacol.

2.5. Hydrodeoxygenation of lignin and suberin derivatives

The residue which remained after distillation possessed twice lower oxygen content than the initial material. In order to fully remove the oxygen and thus convert the oil into hydrocarbons, we subjected the oil to hydrotreatment. Typical monometallic catalysts Pd/C and Pt/C were successfully tested in the reaction with model compound stearic acid (provided heptadecane and octadecane as products) but showed no reactivity in the case of the actual mixture.

We decided to avoid an extensive screening of catalysts since the goal of our study was to show a novel concept of bark valorization but not a detailed optimization of the conditions. Therefore, we considered the recently reported bimetallic Pt-MoO$_3$/TiO$_2$ catalyst which was previously shown to be efficient for hydrodeoxygenation reactions.[51] The catalyst was prepared according to the literature procedure except that it was not reduced prior to the reaction. Hydrodeoxygenation was carried out for 20 h at 350 °C with 50 bar of hydrogen gas. The product was subjected to distillation in Kugelrohr to afford colorless or yellowish oil (42 wt.% of initial bark weight). The obtained hydrocarbon oil was analyzed using a number of techniques.

2.6. 2D GC analysis of the hydrocarbon bio-oil

Using 1D GC afforded to identify some of saturated hydrocarbons with high carbon atom numbers. However only two-dimensional gas chromatography (2D GC) technique made it possible to get an insight into the precise composition of the mixture.

2D GC (see Appendix) implements a system of two connected columns of different polarity.[55] The flow which leaves the first column is trapped with a modulator which is located in between the columns. The modulator collects fractions over certain periods of time before injecting them into the second column. The resulting chromatogram is represented in a two-dimensional form using a specialized software. The retention times on each axis are usually correlated with polarity and boiling point.

In this study, 2D GC (Figure 6, Table 2) made it possible to distinguish between *n*-alkanes, isoalkanes, alkenes, and other types of structurally similar compounds contained in the complex mixture. Therefore it also allowed to derive average molecular formulas for each type of compounds and for the mixture as a whole. The following expressions were used for the calculation:

$$x_i = \frac{\sum_A n_i(A)\nu(A)}{\sum_A \nu(A)} \qquad \text{(Eqn. 1)}$$

$$\omega_i = \frac{\sum_A n_i(A)\nu(A)M_i}{\sum_A \nu(A)M(A)} \qquad \text{(Eqn. 2)}$$

where x_i and ω_i are molar and mass fractions of element i in the bio-oil, $n_i(A)$ is the number of atoms of element i in the component A of the bio-oil, $\nu(A)$ is molar content of A in the bio-oil, M_i is molar weight of element i, $M(A)$ is molar weight of A.

The most abundant compounds found in the reaction mixture were C_8–C_{27} n-alkanes (33%) of the average molecular formula $C_{16.9}H_{35.8}$. In the range of carbon atom numbers from 10 to 21, the distribution of n-alkanes was rather wide and the content of each compound was 0.7–1.6%.

The second largest type of compounds were cycloalkanes and alkenes with the average formula $C_{13.8}H_{27.6}$, comprising 26% of the mixture. Composition of this group is relatively shifted toward lower carbon atom numbers.

Each of the other types of compounds (isoalkanes, alkylbenzenes, naphtalenes, etc.) does not constitute more than 12% of the mixture. The average composition is $C_{14.9}H_{28.4}O_{0.00–0.06}$, i.e. the residual oxygen content is less than 0.5 wt.% (Table 3).

Heat of combustion (the higher heating value, HHV) of the bio-oil was estimated with according to the formula: $HHV = a_C\omega_C + a_H\omega_H + a_O\omega_O$ with various increments known from literature. The values of a_i increments and the HHV values are given in Table 2. The higher heating value estimated for this composition using several linear formulas is 46–49 MJ·kg^{-1}.

Table 2. Estimated HHV (MJ·kg^{-1}).

a_C	a_H	a_O	HHV
33.83	144.28	−14.05	**47.9…48.2**
35.17	116.25	−11.10	**45.4…45.7**
33.62	141.93	−14.53	**47.4…47.8**
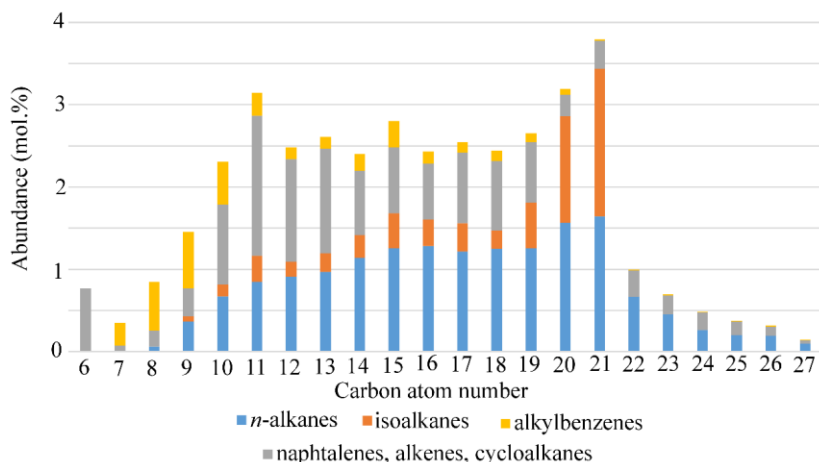
Figure 6. Composition of the hydrocarbon bio-oil (2D GC data).

Table 3. Composition of the bark-derived hydrocarbon bio-oil.

Type of compounds	Content, mol. %	Average molecular formula
n-alkanes	32.6	$C_{16.9}H_{35.8}$
iso-alkanes	12.3	$C_{17.3}H_{36.7}$
Cycloalkanes and alkenes	25.9	$C_{13.8}H_{27.6}$
Alkylbenzenes	7.7	$C_{11.6}H_{17.2}$
Tetralins, indans and naphtalenes	11.1	$C_{11.7}H_{14.5}$
Higher aromatics	4.5	$C_{14.5}H_{11.1}O_{0.06}$
Others	5.9	–
Total	100.0	$C_{14.9}H_{28.4}O_{0.00-0.06}$

2.7. Simulated distillation

Simulated distillation is a GC (see Appendix) method which allows to estimate the boiling range distribution of a small sample without performing a large-scale distillation of a bulk material.[56] Samples are subjected to GC in a non-polar column and the retention times are correlated with boiling points. For the latter, a calibration curve is used which is obtained by testing of a known mixture of hydrocarbons, usually *n*-alkanes of the expected boiling point range, under the same conditions.

The results of simulated distillation are given in the form of function which correlates the eluted portion of sample with the established boiling points, just

as in the case of usual large-scale distillation. Thus, the simulated distillation is rapid and efficient analytical tool which is widely used for the petroleum analysis.

In this study, the results of simulated distillation (standard IP480 method; Figure 7) were in accordance with the 2D GC data. The oil includes about 20% of products of gasoline boiling point range (<200 °C), 45% of diesel (200–300 °C), 33% of heavy gas oil (300–420 °C), and only 2% of non-volatile waxes (>420 °C). For the range 161–380 °C and 8–93% of distilled material, the distillation curve is described by the linear equation: wt.% = $0.43 \cdot T°C - 63.9$, with $R^2 = 0.996$. Heavy low-volatile hydrocarbons representing one third part of the obtained material may be used as lubricants or subjected to the further cracking to yield fractions of fuel range.
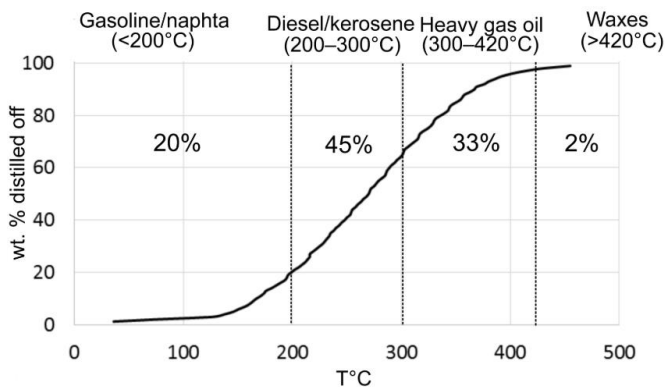
Figure 7. Simulated distillation of the hydrocarbon bio-oil.

2.8. Van Krevelen plot of the process

Van Krevelen plot depicts the ratios of hydrogen, oxygen, and carbon in a studied sample, typically of coal or petroleum nature.[57] The vertical axis stands for H:C ratio and the horizontal axis for O:C ratio. We used this type of representation to show the transformation of bark material throughout the process (Figure 8). The plot was built according to the elemental analysis (for the products of the stages 1 and 2) and 2D GC data (for the product of stage 3).

The initial bark sample itself was oxygen-rich (H:C = 0.45, O:C = 1.45). First stage of the process decreases the oxygen content, thus the O:C ratio for the obtained intermediate oil is only 0.27. The residue after distillation possesses slightly higher O:C ratio, probably due to condensation and dehydration processes. The final reduction subtracts the oxygen, leading to the hydrocarbon oil with an close to zero O:C ratio.
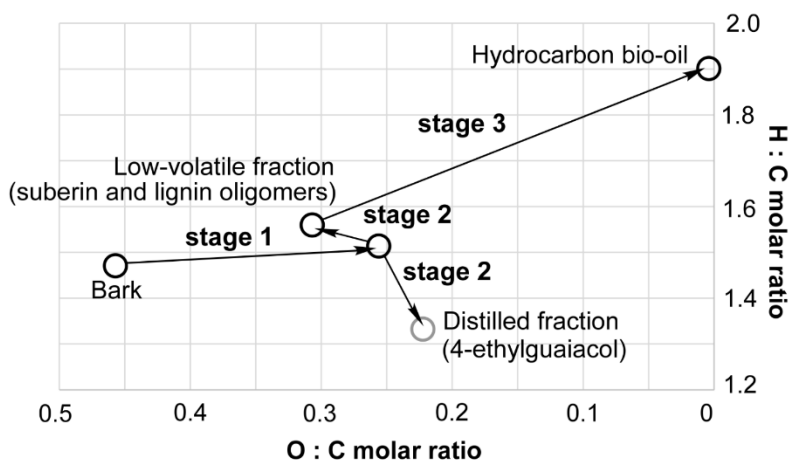
Figure 8. Van Krevelen plot for the developed process of bark valorization.

2.9. Summary

Lignin-first methodology could not be applied directly to bark because of the presence of suberin. Instead, slightly basic conditions were required to depolymerize both suberin and lignin. Under these conditions, the bark was converted into a mixture of monophenolic compounds, oligomers from lignin, and fatty acids and oligomers from suberin. 4-ethylguaiacol (**1**) (2.6% of bark weight, 90% purity) could easily be distilled off. The resulting mixture was then hydrodeoxygenated to generate a hydrocarbon bio-oil (42% of bark weight). The carbohydrate domain is partially consumed and serves as a source of hydrogen in the initial reaction of the lignin cleavage implemented at the first stage of the process.

The obtained oil was studied with GC-MS, 2D GC, and Simulated distillation techniques, and was shown to contain a variety of hydrocarbons (alkanes, alkenes, cycloalkanes, aromatics) of 6 to 27 carbons. The average composition is $C_{14.9}H_{28.4}O_{0.00-0.06}$ (less than 0.5 wt.% of the residual oxygen). The estimated higher heating value for this composition is 46–49 MJ·kg^{-1}.

Thus, bark has been shown to have potential as a renewable feedstock of chemicals and fuels.

3. Conversion of birch bark to biofuels in a recyclable solvent system (paper II)

3.1. Background

The process described in the previous chapter, though allowing to separate and valorize the components of bark, possesses sufficient drawbacks. First, the utilization of nonvolatile ionic compound, sodium hydroxide, does not allow to recycle the solvent. Second, the palladium catalyst is also scarcely recyclable because of the mixing with bark residue. Therefore, this process cannot be implemented at the industrial scale.

To get closer to an environmentally friendly and cost-efficient scheme, we decided to replace sodium hydroxide with a volatile base triethylamine and focus on complete hydrodeoxygenation of the extract instead of isolation of lignin monomers.

3.2. The process overview

In the upgraded version of the process, we moved from the bark of oak (*Quercus suber*) to the bark of birch (*Betula pendula*). The latter is produced as waste in Swedish pulp mills, the annual quantity reaching 1.5 million tons. Therefore this feedstock is more representative of Swedish conditions and is more interesting practically.

The bark was treated with MeOH–H_2O–Et_3N mixture at 160–220ºC in a stainless steel reactor (Scheme 8). In these conditions, trimethylamine works as a base and deprotonates water to generate hydroxide anions, which in turn can cleave the ester linkages of suberin. Methanol then solubilizes the released fatty acids. After the reaction, the insoluble bark tissues (7%) are filtered off. The solvent is evaporated from the filtrate and collected. The residue can be directly hydrotreated under the conditions which are described in chapter 2.
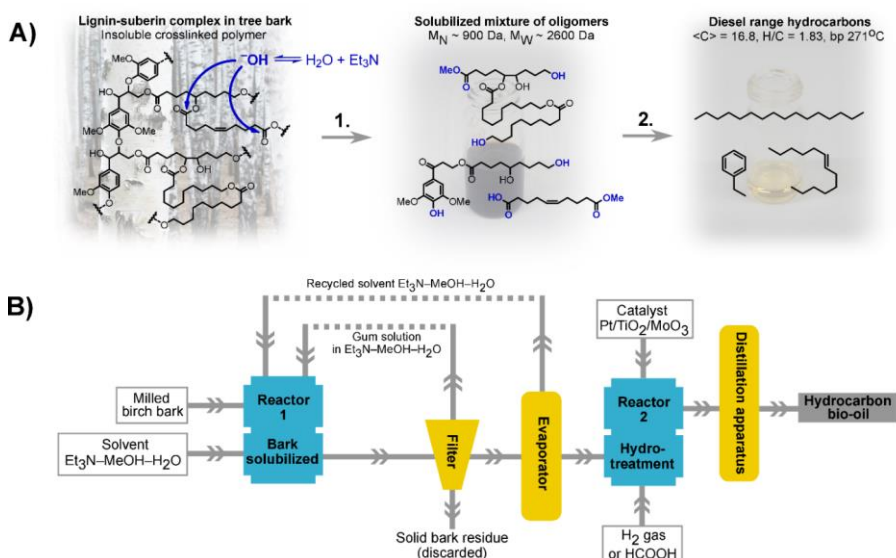
Scheme 8. A) Chemistry of the bark conversion to biofuel. B) Scheme of the procedure.[i]

3.3. Solubilization of bark in MeOH–H₂O–Et₃N solvent system

Water and alcohols at 300 °C – 400 °C can solubilize plant biomass in the absence of catalyst. However, the necessity to heat the solvent to these temperatures would create a prohibitive additional demand of 10–20 MJ per kilogram of the biofuel product and make it necessary to use a high pressure equipment. In the present procedure, Et₃N catalyst enables suberin depolymerization and thus allows to run the process at 200 °C and to avoid extra expenditures.

The optimal conditions for solubilization of bark at the first step were found with the focus on minimization of the mass of insoluble tissues (Figure 9). The degrees of solubilization (%) are reported here in relation to the mass of extractive-free bark (EtOH extractives plus water content of 29%). As a starting point, the bark was treated with MeOH–H₂O (1:1 v/v or 46% volume fraction of H₂O) at 220 °C for 1 h in the absence of Et₃N. Without a catalyst, only 27% of the bark was solubilized. Addition of Et₃N (4% volume fraction) improved the results and 69% of the bark was solubilized. Increasing the volume fraction of Et₃N to 7% gave 91% solubilization of the bark. A further increase in the Et₃N volume fraction (12%) caused a decrease in the solubilization degree (73%). Using the optimized Et₃N volume fraction (7%), the role

of water in the solvent mixture was explored. If no water was added (i.e., a Et_3N–MeOH mixture was used), the solubilization degree was lower than that obtained with MeOH–H_2O 1:1 v/v, but still relatively high (70%). Addition of water (30% volume fraction) did not greatly improve the solubilization (72%). When water became the major component at a volume fraction of 60%, the degree of solubilization reached a maximum (93%). Use of the H_2O–Et_3N system without MeOH led to a small decrease in the degree of solubilization (89%); however, the resulting mixture was difficult to handle during filtration. For optimal solubilization and separation, a MeOH volume fraction of 46% was used. The effect of temperature was also investigated. When the process was carried out for 1 h with the optimized solvent system (MeOH–H_2O 1:1 v/v, 7% volume fraction of Et_3N) at 160 °C, poor solubilization was observed (13%). Increased temperature afforded better results with degrees of solubilization of 45% at 180°C, 54% at 200°C, and 91% at 220°C.
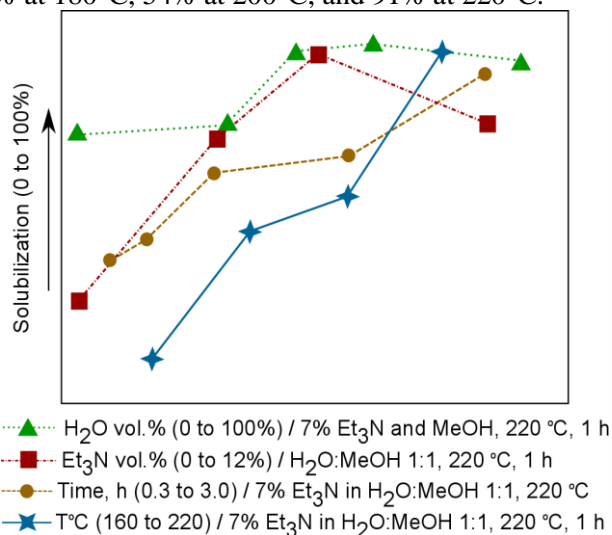
Figure 9. Optimization of conditions for bark solubilization.[ii]

The gum obtained from this extract after removal of the solvent was studied by means of size-exclusion chromatography, elemental analysis, NMR and gas chromatography. The oligomeric products of cleavage of suberin and lignin had average molecular weights $M_W = 2630$ Da and $M_N = 932$ Da (PD = 2.8). This means that the average dissolved molecule was composed of 4–5 monomeric units of lignin and/or suberin. The elemental composition (C, 66.7% // H, 10.2% // N, 2.1% // O, 21.4%) was similar to that of the initial bark. The gum was dispersable in hexane, moderately soluble in toluene (28% of the mass), and readily dispersable in methanol (87% of the mass). Notably, it became miscible with tall oil fatty acids at 120 °C, and the suspension remained stable at room temperature. The viscosity of the suspension was 15–

---

500 mPa·s for the mass fraction range of 7%–33% and temperatures 25°C–70°C. Therefore, biomass-derived tall oil fatty acids can be used as a carrier liquid in industrial gum hydrotreatment processes, as shown previously for kraft lignin acylated with fatty acids.[58]

HSQC NMR results (Figure 10, A) demonstrated the presence of typical structural motifs of suberin and were in accordance with previous data obtained for birch bark.[13] To analyze the monomeric fatty acids, the gum was subjected to alkaline methanolysis and the extract was studied by GC (Figure 10, B). A variety of C_{16}–C_{22} hydroxylated carboxylic acids and diacids were identified,[59,60] with the main components being 22-hydroxydocosanoic acid (26% TIC as silylated derivative) and 1,18-octadec-9-enedioic acid (14%). In addition, ferulic acid (3%) was detected.
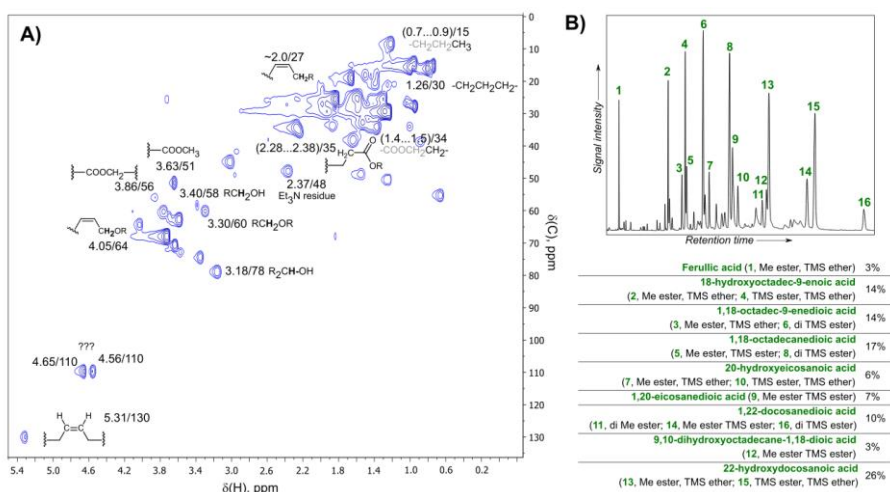
Figure 10. Analyses of bark-derived gum by A) HSQC NMR and B) by GC-MS of methanolysate.

3.4. Hydrodeoxygenation of the extract

The mixture of solubilized lignin and suberin was hydrotreated in the presence of $Pt/MoO_3/TiO_2$ catalyst which was tested in the previous project. At the lab scale, the reaction is run in neat, which makes the analysis of products easier. However, the gum was shown to be miscible with tall oil fatty acids: the mixtures possess convenient viscosities 10–500 mPa·s at 25–70ºC and can be used as feeds in a hydrotreater.

Composition of the obtained biofuel was initially studied by means of simulated distillation (see Appendix). As in the previous project, the mixture was shown to be composed of hydrocarbons within the aviation and road fuel ranges, with the initial boiling point 70 °C and 90% of the mixture boiling below 350 °C (Figure 11, A). Further analysis with 2D GC (see Appendix)

allowed to discover various classes of compounds present in the mixture (Figiure 11, B). The whole range of hydrocarbons from C7 to C26 has been found, with the maximum abundance for C15–C19. It should be noted that the initial suberin fatty acids have only even carbon numbers: cracking and decarboxylation are the possible reasons for the presence of compounds with uneven carbon numbers in the biofuel. Highly unsaturated yet low-molecular-weight hydrocarbons such as benzenes and naphtalenes (20% mass fraction) can also be products of cracking. In total, unsaturated compounds comprise 73% of the mixture by mass; and the average number and/or cycles per molecule for the whole mixture is 2.4 and the H/C ratio is 1.83. The theoretically estimated higher heating value of the biofuel is 45.4–48.2 MJ kg^{-1} (average of 46.5 MJ·kg^{-1}).
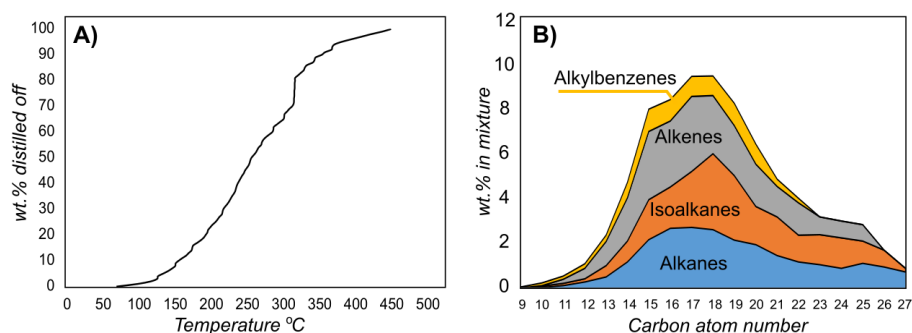
Figure 11. A) Simulated distillation, B) 2D GC of the bio-oil.

3.5. Recycling of the solvent

When the mixture becomes too viscous to be used for solubilization of more bark, the solvent should be recycled by distillation at about 100 mbar (water pump). The maximum normal boiling point is 90ºC (triethylamine), therefore almost quantitative evaporation can be accomplished. Efficiency of recycling was estimated by analyzing the composition of the mixture after each run by means of ^{1}H NMR in acetone-d$_6$. The concentration of Et$_3$N slightly decreased after each distillation. This did not have large impact on the results of further reactions (Table 4). As the major loss was observed in the first distillation, we assumed that the equipment might be saturated with volatiles.

Table 4. Recycling of the solvent by evaporation.

№ of run	Solvent composition (vol.%)			Solvent recovery (wt.%) [compared to initial mass]	Bark solubilization (wt.%)
	Et$_3$N	MeOH	H$_2$O		
1	7	47	46	94 [94]	91
2	6	49	45	99 [93]	92
3	6	48	46	99 [92]	87
4	6	40	54	–	89

3.6. Estimation of the energy demand

Table 5. Parameters used for the estimation of energy demand

Symbol	Meaning	Value	Units	Estimation method
V	volume of the solvent per kg of bark feedstock (stage 1)	8–10	L·kg^{-1}	experiment
Y	yield of the bio-fuel per kg of bark feedstock (stage 2), $0 < Y < 1$	0.4	dimensionless	experiment
Q_1	vaporization heat of the solvent (stage 1)	1.48	MJ · L^{-1}	calculated additively
Q_2	vaporization heat of the bio-fuel (stage 2)	0.31	MJ · kg^{-1}	vaporization enthalpy of hexadexane
C_1	heat capacity of the solvent (stage 1)	$2.86 \cdot 10^{-3}$	MJ · K^{-1} · L^{-1}	calculated additively
C_2	heat capacity of the bio-fuel (stage 2)	$2.21 \cdot 10^{-3}$	MJ · K^{-1} · kg^{-1}	heat capacity of hexadecane
T_{b1}	boiling point of the solvent (stage 1)	< 358	K	calculated through Raoult law
T_{b2}	boiling pouint of the bio-fuel (stage 2)	< 553	K	calculated from Simdis and 2D GC data
C_r	heat capacity of the reactor material	$5 \cdot 10^{-4}$	MJ · K^{-1} · kg^{-1}	heat capacity of stainless steel
m	mass of the reactor divided by the bark mass	see *Estimation method*	dimensionless	[a]
S	surface area of the reactor divided by the bark mass	see *Estimation method*	m^2 · kg^{-1}	[b]
w	coefficient of heat transfer between the reactor and air	10^{-3}	MJ · m^{-2} · K^{-1} · min^{-1}	coefficient of heat transfer between the stainless steel and air
t_1	reaction time (stage 1)	120	min	experiment
t_2	reaction time (stage 2)	120	min	experiment
T_{r1}	reaction temperature (stage 1)	493	K	experiment
T_{r2}	reaction temperature (stage 2)	643	K	experiment
n_C	number of reaction cycles proceeding without cooling down the system	1–20	dimensionless	different values are considered, see Table 6
n_S	number of reaction cycles proceeding without evaporation or replacing the solvent	1–3	dimensionless	different values are considered, see Table 6
D_1	energy required for distillation of the solvent (stage 1)	(to be calculated)	MJ per kg of the bio-fuel	
D_2	energy required for distillation of the bio-fuel (stage 2)	(to be calculated)	MJ per kg of the bio-fuel	
H_1	energy required for heating of the reactor (stage 1)	(to be calculated)	MJ per kg of the bio-fuel	
H_2	energy required for heating of the reactor (stage 2)	(to be calculated)	MJ per kg of the bio-fuel	

[a] $\quad m \approx \frac{4.17 \rho_R}{x} \cdot ((0.24x/\rho)^{1/3} + \Delta r)^3 - \frac{\rho_R}{\rho}$

x [kg] is loading of the bark feedstock, $\rho_R = 8 \cdot 10^3$ [kg · m^{-3}] is density of stainless steel, $\Delta r = 0.01 \ldots 0.05$ [m] is thickness of the reactor wall, $\rho = 150$ [kg · m^{-3}] is density of bark packing in the reactor

[b] $S \approx \frac{12.56}{x} \cdot ((0.24x/\rho)^{1/3} + \Delta r)^2$

x [kg] is loading of the bark feedstock, $\Delta r = 0.01 \ldots 0.05$ [m] is thickness of the reactor wall, $\rho = 150$ [kg · m^{-3}] is the density of bark packing in the reactor

Energy [MJ for producing 1 kg of the biofuel]
$$= H_1 + D_1 + H_2 + D_2 \qquad \text{(Eqn. 3)}$$

$$D_1 = (Q_1 + C_1 \cdot (T_{d1} - 293)) \cdot V/(Y \cdot n_S) \qquad \text{(Eqn. 4)}$$
$$D_2 = Q_2 + C_2 \cdot (T_{d2} - 293) \qquad \text{(Eqn. 5)}$$

$$H_1 = (C_1 \cdot V + C_r \cdot m/n_C + S \cdot w \cdot t_1) \cdot (T_{r1} - 293)/Y \qquad \text{(Eqn. 6)}$$
$$H_2 = (C_2 \cdot Y + C_r \cdot m/n_C + S \cdot w \cdot t_2) \cdot (T_{r2} - 293)/Y \qquad \text{(Eqn. 7)}$$

To get an insight into the conditions which would make the process cost-efficient, energy demand of the process has been roughly estimated. Four principal summands were considered, corresponding to heating and distillation of the reaction components at both stages (Table 5 and Equations 3–7). Other energy inputs were assumed to be negligible.

The energies H_1 and H_2 required for heating of the reaction mixture at each stage include contributions from the increase of temperature of the reaction mixture and the reactor and from maintaining the required temperature. Similar contributions there are in the case of distillation energies. Table 6 shows that stage 1 has the main influence on the energy demand, shared equally between heating and distillation. Energy efficiency of the process can be defined as the difference between the heat of biofuel combustion (ca. 46 MJ kg^{-1}) and the energy required for it's production. The calculation reveals that the process becomes energetically efficient only at the industrial scale, for several tons of bark loading and with efficient recycling of the solvent.

Table 6. Theoretically estimated energy demand of the described process with variable parameters.

n_C	n_S	x [kg]	V [L·kg^{-1}]	Energy demand for each step [MJ · kg^{-1}] (with % of total)								Total energy demand [MJ · kg^{-1}]
				H_1	%	D_1	%	H_2	%	D_2	%	
1	1	1	10	36	31	42	35	40	33	1	1	119
1	1	10^3	10	16	26	42	67	4	6	1	1	62
1	1	10^4	10	15	25	42	70	2	4	1	2	60
10	1	10^3	10	15	25	42	71	2	3	1	2	59
10	3	10^4	10	15	47	14	44	2	5	1	3	31
10	3	10^4	7	11	46	10	43	2	7	1	4	23

3.7. Estimation of the environmental impact

With the data on conditions and energy demand of the optimized process in hand, we evaluated its environmental benefits and drawbacks using a methodology of Life Cycle Asessment (LCA). LCA follows the framework stand-

ardized by ISO 14040. As the result of this calculation, one gets a set of impacts expressed in different units such as kg of Cu equivalents for metal depletion or kg of SO_2 equivalents for terrestrial acidification.

The principal stages and components of the process which were included in the assessment are shown in Figure 12. The feedstock supply section includes the materials used in the procedure (bark chips, methanol, trimethylamine, water, catalyst) as well as the heat energy and fuels for transportation. The section for conversion includes all operations undertaken with the feedstock; solubilization, filtration and distillation, bark residue incineration, wastewater treatment and hydro-deoxygenation treatment. For comparison, a similar assessment for fossil-based diesel production was performed, based on the steps of extraction of crude oil, distillation/fractionation of crude oil, and treating processing for production of diesel. The combustion energies for biofuel and fossil-derived fuel were assumed to be equal.
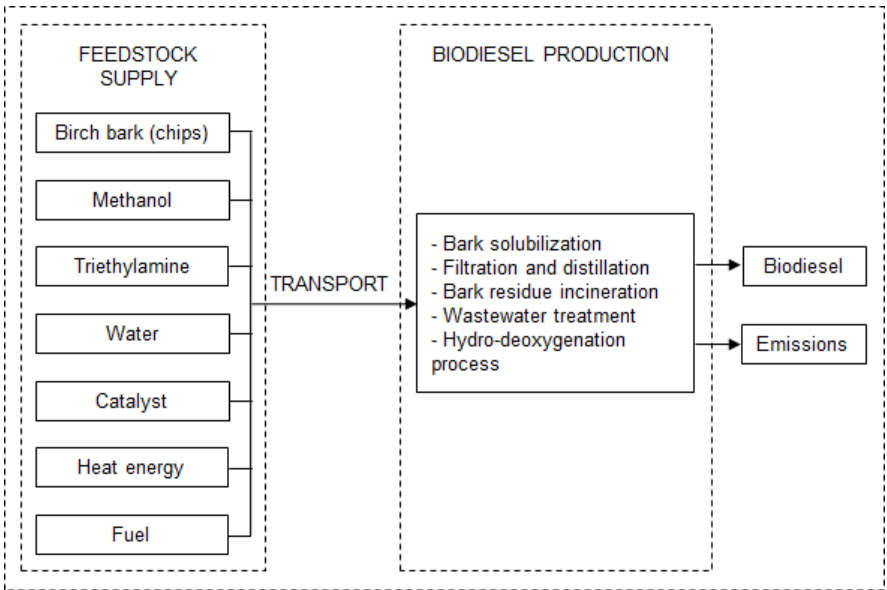

Figure 12. Stages and components of the process included in the assessment

To find possible improvements for the process, four scenarios have been examined in this environmental assessment (Table 6). In the Scenario 1, the process is considered stand-alone and continuous. The solvent is recycled and continuously added back to the reaction. Energy is supposed to come from burning of natural gas. In this scenario, biofuel was found to have less environmental impact than the fossil-based fuel only in the following categories: fine particulate matter formation, fossil depletion, freshwater consumption, ionizing radiation, marine eutrophication, photochemical ozone formation, stratospheric ozone depletion, and terrestrial acidification. Climate change,

freshwater eutrophication, land use, human toxicity, metal depletion, and freshwater, marine, and terrestrial ecotoxicity are the categories where the proposed process, under scenario 1, turned out to have worse properties than the fossil-based production. In particular, in this case the process would produce 1.7 kg of CO_2 eq. of greenhouse gas emissions for 1 kg of biofuel.

Table 6. Scenarios for the environmental performance assessment of birch bark conversion into biofuel

Scenario	Description
# 1	**Baseline, continuous process** Reaction in a continuous process. Milled bark is treated in the solvent and the mixture is filtered. The filtrate, which includes solubilized bark, is returned to the system to play the role of solvent for the next portion of feedstock. After two runs recirculating the solvent, the filtrate becomes viscous and it is then distilled to recover the solvent for subsequent reactions. New solvent is continuously added to substitute the solvent loss of 2% by volume per distillation. Natural gas is the source of heat energy.
# 2	**Electricity mix as input for heat energy, Europe** Reaction in a continuous process (baseline). The average electricity mix of Europe, mostly based on fossil fuel electricity generation, is the source of heat energy.
# 3	**Electricity mix as input for heat energy, Sweden** Reaction in a continuous process (baseline). The average electricity mix of Sweden is the source of heat energy. Sweden was chosen for this scenario as an example of a country with electricity production based on low-carbon technologies (mainly hydropower and nuclear power).[61]
# 4	**Heat energy and methanol as waste streams of paper and pulp industry** The best-case scenario specifically for countries like Sweden, where excess heat and methanol from the paper and pulp industries can be used in the bark valorization process. The environmental impacts of these two feedstocks are thus considered zero.

Scenarios 2 and 3 are similar to the first one but heat is supplied by electricity instead of combustion of natural gas. Under the second scenario, electricity from the sources typical for Europe is assumed to be used. This scenario relies largely on fossil fuel, therefore it has even higher environmental impact

than the first one. Scenario 3 which implements Swedish energy sources–hydropower and nuclear power–also has big impacts in the categories for ionizing radiation and land use, however, it performed better than the other two scenarios when pertaining to climate change, fine particulate matter formation, and terrestrial acidification.

In comparison with the fossil-based diesel production, scenarios 2 and 3 can be benefitial in the categories of formation, terrestrial ecotoxicity, climate change (the greenhouse gas emissions decrease to 0.495 kg of CO_2 eq. in the scenario 3), fine particulate matter formation, fossil depletion, stratospheric ozone depletion, and terrestrial acidification. In other categories, the usual fossil-based diesel still showed better results.

In the scenario 4, the process of bark valorization is interconnected with the existing facilities of pulp industry. It is the best-case scenario which is feasible in the areas close to pulp mills which can supply the excess heat and methanol. Therefore the environmental impacts associated with the corresponding stages of the process will be negligible. In comparison with the fossil-based diesel production, Scenario 4 has lower impact in all categories except freshwater eutrophication, human toxicity, and metal depletion. The GHG emissions are decreased to −0.06 kg of CO_2 eq. In this case, the land use would be also close to null because the bark can be collected as waste product of the pulp mill, as well as the most of other environmental impacts included in the assessment.

3.8. Summary

In this project, a process for solubilization and hydrodeoxygenation of birch bark was developed. For the solubilization stage, we used a recyclable, salt and metal-free solvent system of MeOH–H_2O–Et_3N with triethylamine as a basic catalyst for hydrolysis of ester bonds in the bark tissue. For hydrodeoxygenation, we treated the solubilized lignin and suberin with hydrogen gas in the presence of Pt catalyst. As the product, a fuel within the gasoline–aviation–diesel range was obtained with a 40% yield from the initial bark mass. At the lab scale, the process is not energetically efficient nor green enough, however, at the industrial scale it is expected to become affordable, requiring only 23 MJ of energy to yield 1 kg of diesel product.

To get an insight into the potential environmental impact of this technology, a Life Cycle Assessment has been performed, taking into account different scenarios which can take place upon implementation of the process in industry. Various categories of impacts were considered, and the only categories in which the conventional fossil-derived fuel is definitely more beneficial than the biofuel are freshwater eutrophication, human toxicity, and metal depletion.

4. Lignin depolymerization to monophenolic compounds in a flow-through system (paper III)

4.1. Background

As mentioned previously, the lignin-first approach offers a number of advantages as a biomass fractionation strategy. In particular, it allows to capture high-value lignin products directly after the depolymerization.

However, the majority of the developed procedures also have substantial drawbacks. Typically they require to mix heterogeneous metal catalysts with a solid biomass in one batch reactor. As a result, the fractionation becomes complicated with respect to catalyst recovery, mass transfer, and pulp contamination with the catalyst; external hydrogen and other additives (for instance, trapping agents for lignin monomers) are sometimes needed. These problems limit applicability of the method.

The goal of this study was to separate the pulping and the catalytic stages in space and time and to investigate the mechanism of the reactions taking place in the lignin-first process, i.e., to establish the individual roles of the solvent and the catalyst.

4.2. The flow process overview

In order to overcome the mentioned drawbacks, we have envisioned a process in which the biomass pulping and the catalytic transfer hydrogenolysis are separated in space and time and the mass transfer is accomplished by the flow of a solvent mixture. The arrangement of the equipment and some details of the procedure are shown in Scheme 9. The first cartridge contains the biomass to fractionate (milled birch wood). The second cartridge is loaded with the catalyst (Pd/C, 5 wt.%). Both cartridges are plugged with filters in order to keep solids inside. A preheater is installed before each cartridge: this guarantees that the solvent flow enters the cartridge at the desired temperature. In order to study the first step of the process separately, the system can be assembled with only one cartridge. In the end of the line, a back pressure regulator (BPR) is installed to prevent solvents from boiling.

Once the reactor is assembled, the solvent system is streamed at a certain flow rate using an HPLC pump. After all of the components are moistened with solvent, the heat is applied (temperatures of cartridges and corresponding

preheater are marked as T_1 and T_2) and the emanating solution of products is collected.

The workup of the mixture is carried out by diluting with DCM and water and collecting the organic phase which contains lignin-derived products. The aqueous phase containing residual carbohydrates is also analyzed. The pulp is recovered from the first cartridge and enzymatically converted into glucose.
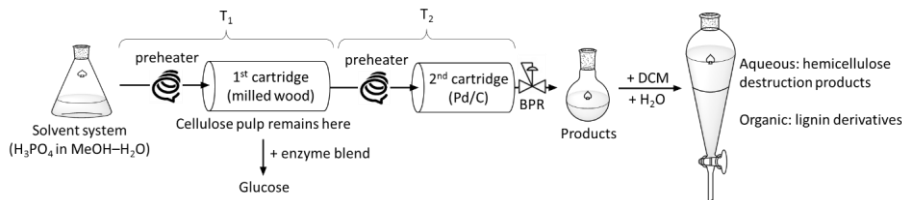
Scheme 9. The flow process

4.3. Optimization of the reaction conditions

The reaction conditions were optimized by means of the yield of lignin-derived monomeric phenolic compounds which are the most valuable products of the process (Figure 13). MeOH–H_2O solvent system was chosen which is typical for organosolv pulping. It was shown recently that the acidic reaction conditions are more favorable than the alkaline ones for the cleavage of lignin toward monomeric compounds,[40] and therefore we focused on acidic media which was created by addition of phosphoric acid to the solvent system.
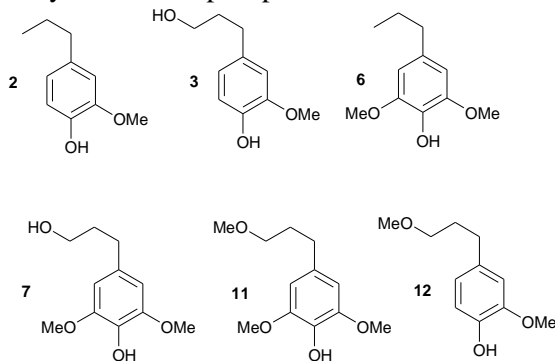

Figure 13. The main phenolic products of the flow process.

Several parameters have been varied: H_2O content in the mixture; concentration of H_3PO_4; temperatures T_1 and T_2; flow rate r; reaction time. Independent variation of all parameters would require a huge number of runs, therefore we optimized them one by one, using the data found on each step for the subsequent step.

Initially, the reactions were run in methanol without water addition, with $T_1 = 200\ °C$, $T_2 = 180\ °C$, $r = 0.2\ mL \cdot min^{-1}$. This system afforded poor yields,

however the concentration of H_3PO_4 was optimized. Under variation of concentration from 0 to 10 g·L^{-1} the yield increased from 0 to 6% with an optimum of 9% at 2.8 g·L^{-1}.

Then, we examined the effect of composition of solvent mixture. Upon dilution of methanol with water, the yields of the phenolic monomers raised gradually until the concentration of water reached 30 vol.%. Further dilution (50 vol.%) caused a decrease of the yields.

Some of the results from the temperature optimization are presented in the Table 7 (see SI of the paper II, section 4.2, for more comprehensive data). Starting point with $T_1 = T_2 = 180$ °C and $r = 0.2$ mL·min^{-1} (entry 1) provided monomer yield of 17%. Increasing T_1 to 200 °C resulted in improvement of the yield to 27% (entry 2). Further raise T_1 to 220 °C, however, led to a drop in yield to 24% (entry 3). Similarly, variation of T_2 from low to high values (160 to 200 °C, entries 1, 4, 5, yields 22 to 27%) showed that the T_2 optimum is in between (180 °C). After optimization of both T_1 and T_2 (200 and 180 °C), we have varied flow rates from 0.1 to 0.5 mL·min^{-1} (entries 2, 6, 7, 8).

The flow rate 0.1 mL·min^{-1} resulted in zero yield of phenolic monomers, presumably because of over reduction. On the other hand rate of 0.5 mL·min^{-1} afforded the products but the yield (22%) was lower than in the case of $r =$ 0.2 mL·min^{-1}. The optimum was found to be at 0.3 mL·min^{-1} (31% yield of phenolic monomers).

Table 7. Selected points of the process optimization.

En-try #	T_1 (°C)	T_2 (°C)	Flow rate (mL·min^{-1})	Lignin monomers yield (wt %) [a]
1	180	180	0.2	17
2	200	180	0.2	27
3	220	180	0.2	24
4	200	200	0.2	22
5	200	160	0.2	22
6	200	180	0.3	31
7	200	180	0.5	21
8	200	180	0.1	0
9 [b,d]	200	180	0.3	29
10 [b]	200	180	0.3	39 (37 [c])

Reaction conditions: birch wood meal (150 mg, untreated unless otherwise stated), 5 wt% Pd/C (150 mg, ~1:2 Pd:lignin mole ratio), solvent system: 2.8 g·L^{-1} H_3PO_4 in MeOH–H_2O 7:3 v/v.

[a] ^{1}H NMR data, internal standard CH_3NO_2, represented wt% of total lignin.
[b] Solvent-pretreated wood meal (soaked with solvent overnight).
[c] GC-MS data, internal standard tetracosane.
[d] Dewaxed wood meal (EtOH, Soxhlet extractor, then air drying).

Finally, we investigated the effects of the biomass pretreatment. The typical pre-extraction procedure (EtOH in Soxhlet) unexpectedly led to the decrease of the biomass susceptivity to the pulping conditions. The probable reason is that the extraction followed by drying causes modification of the wood fibers, making them less accessible to the pulping solvent. On the contrary, overnight pre-soaking of the biomass with solvent followed by the flow process led to a significant improvement of the monomers yield (39% NMR yield or 37% GC yield, entry 10).

4.4. The reaction mechanism

To study the delignification kinetics, we conducted the reaction in the flow reactor with the second cartridge removed. Therefore, only the first (organosolv pulping) step have been run. The lignin concentration was measured using UV spectroscopy. We have found that the delignification is rapid and becomes almost complete after 60 minutes of the run (Figure 14). As expected, the relative content of lignin with higher molecular weight in the fractions increased over time as shown by SEC (Figure 15, a).
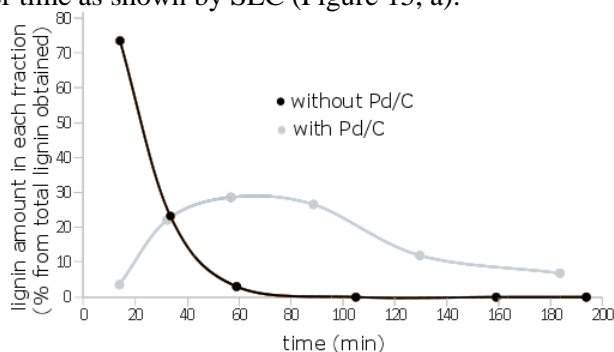

Figure 14. Lignin content in fractions obtained at different reaction times in Pd/C-involving and Pd/C-free flow processes (% from total lignin obtained).

In contrast, the overall process (with two cartridges involved) takes about 3 hours to proceed. The lignin content in the first fractions is neglectable, then it goes through a maximum and gradually decreases (Figure 14). Therefore, the catalyst in the second cartridge plays the role of an adsorbent, detaining lignin derivatives on their way through the system.
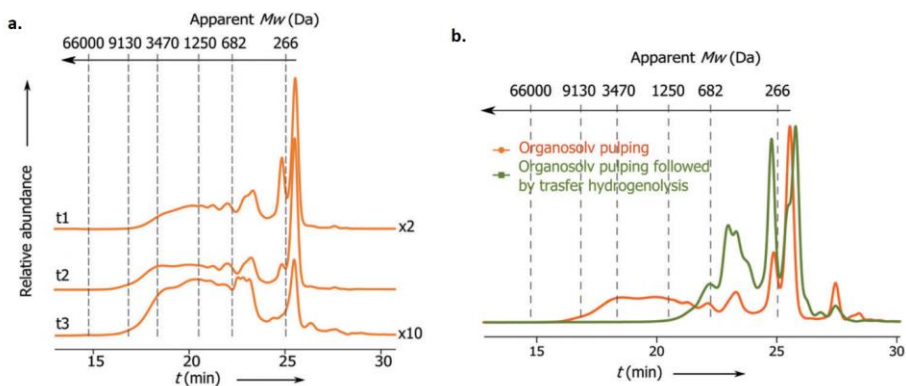
Figure 15. Gradual raise of molecular weight of the lignin removed in the flow organosolv process **(a)** and the comparison of distributions of molecular weights for organosolv and Pd/C-treated lignins **(b)**.

Unexpectedly, the flow procedure allowed to get an insight into the mechanism of the lignin depolymerization under the organosolv conditions. 2D NMR study of products of the first (organosolv pulping) step showed a significant abundance of allylic monolignol moiety among with the expected β-O-4' fragments (Scheme 10, A, B, C). The oxidation state of the allylic moiety is lower than the oxidation state of interunit linkages in the lignin polymer. The yield of two monolignols (methyl ethers of sinapyl and coniferyl alcohols; Scheme 10, F, G) was 15–21% which is higher than the yield which could have been produced by simple leaching of terminal units of lignin chains. This means that some part of lignin is reduced directly during the organosolv process on the first step, before entering the catalyst cartridge.

The conclusion is indirectly supported by comparison of SEC chromatograms of organosolv lignin and Pd/C-treated lignin (Figure 15, b), since the products of low molecular weight are observed in both cases. However, the presence of high molecular weight lignin in the organosolv sample also indicates that the depolymerization was far from completion.

There are two possible reductants which might act in the depolymerization process taking place in the absence of Pd/C catalyst: alcohol and hemicellulose, as we know that cellulose remains untouched. We have conducted a model reaction to investigate which of the two is more likely be the reactant. Reduction of isoeugenol into 4-propylguaiacol in the optimized solvent system in the presence of Pd/C and xylose showed 39% conversion of the starting material while in the absence of xylose the conversion was 7%. Therefore, hemicellulose is more likely to be the reductant than methanol in the employed reaction conditions.

34
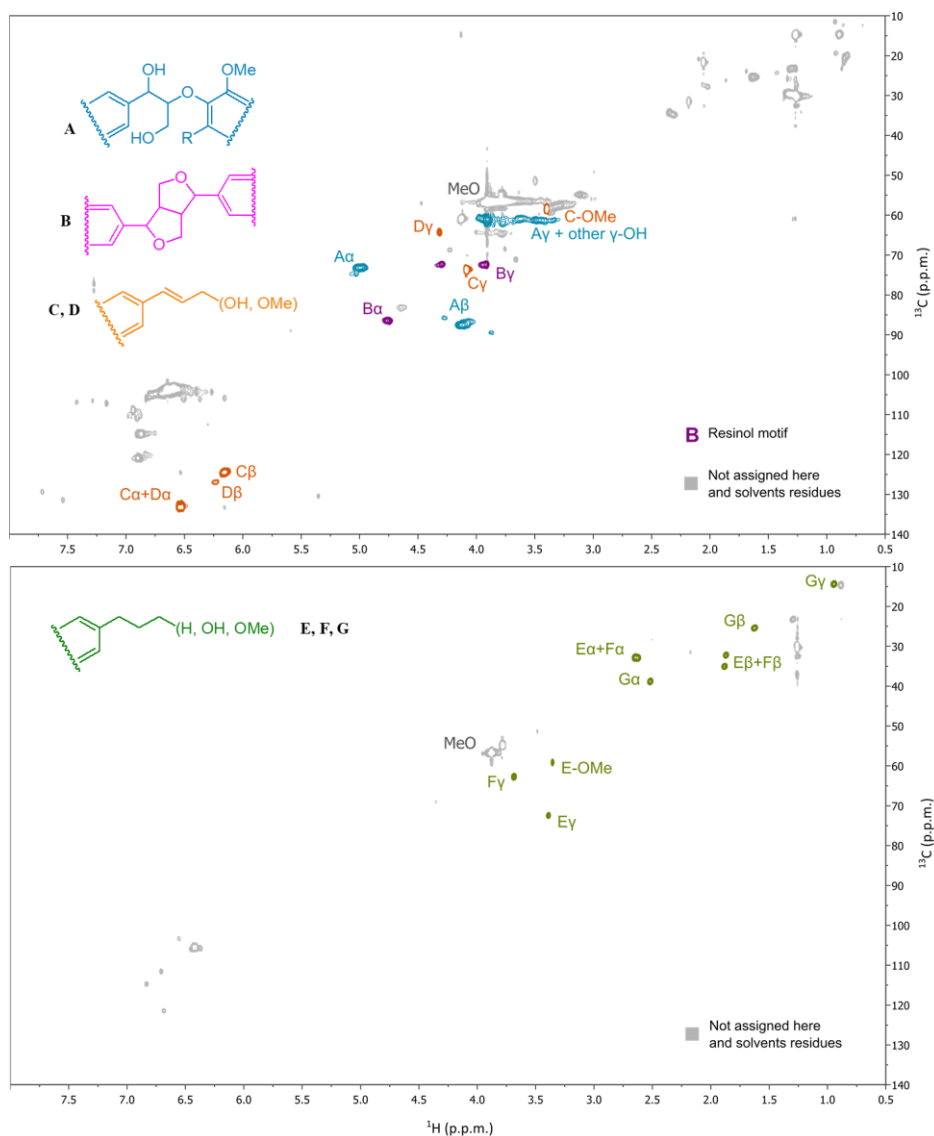
**Scheme 10.** HSQC spectra of organosolv lignin and Pd/C-cleaved lignin obtained in the flow process.

In order to explain the non-catalytic depolymerization of lignin, we have proposed two mechanisms, radical and ionic, based on literature data (Scheme 11). The reduction takes place either due to carbohydrate addition to the α-position of lignin C_3-chain followed by retro-aldol reaction (mechanism 1) or due to the direct transfer of H atom to the radical center of the quinone methide structure (mechanism 2).

4.5. Utilization of carbohydrates

After the pulping is accomplished, 92% of initial amount of wood cellulose remains in the first cartridge in the form of pulp. This cellulose is enzymatically converted into glucose (87% glucose yield, as compared to the initial wood composition). The possibility to achieve enzymatic transformation shows that the pulp possesses high quality: enzymes are typically sensitive to the lignin residue. Moreover, system of two cartridges affords to keep the pulp clean of palladium which may also be poisonous to the enzyme.

On the other hand, hemicellulose is completely degraded during the process, serving as a hydrogen donor for lignin reduction. Neglectable concentrations of the hemicellulose-derived carbohydrates (xylose, methyl-α-D-xylopyranoside, methyl-β-D-xylopyranoside) are found in the aqueous layer after the reaction workup (Table 8).

1.
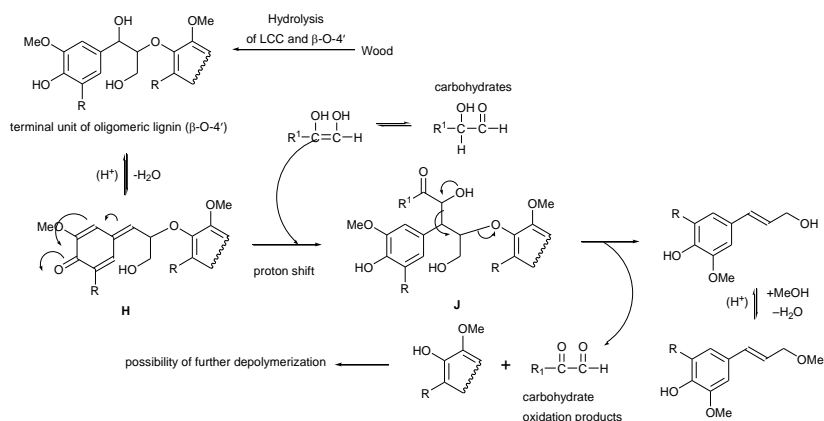
2.
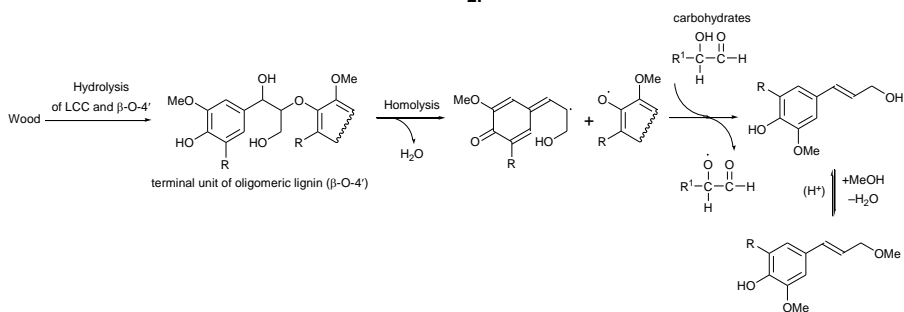
Scheme 11. The two possible mechanisms for depolymerization of lignin taking place in the absence of Pd/C: ionic **(1)** and radical **(2)**.

Table 8. Mass balance of the flow process

	Before the fractionation	After the fractionation	
	Birch wood	Solid fraction	Liquid fraction
Extractives	3	–	–
Xylans	25	0	2 [b]
Glucans	39	35	0
Lignin	23 [a]	1.5	18 [c]
Sum	90	36.5	18
		54.5	

[a] Acid soluble lignin plus acid insoluble lignin
[b] methyl-α-D-xylopyranoside, methyl-β-D-xylopyranoside and xylose
[c] 9% monomers plus 9% oligomers (the latter estimated with SEC data)

4.7. Summary

We have demonstrated that the solvolysis during the pulping and the transfer hydrogenolysis promoted by the transition metal catalyst can be separated in time and space by using flow-through methodology. By separating the two processes, we have been able to distinguish the role of pulping and transition metal catalyzed reactions. Interestingly, and to our knowledge not known, the solvolysis, i.e. pulping is responsible for substantial depolymerization of the lignin polymer and above 20% conversion to monophenolic compounds were observed. The role of the catalyst is dual. One of the roles is to convert highly reactive allylic alcohols from the solvolysis into less reactive species. This is very important to prevent recondensation and thereby affects the monomer yield. The other role of the transition metal is to depolymerize oligomers from the lignin polymer. Thereby, the transition metal transfer hydrogenolysis is required to get high yields of monophenolic compounds (39%). We propose that solvolysis is responsible for cleaving terminal ether bonds by pealing and that the transition metal is responsible for cleaving internal ether bonds. The advantage of using the flow-through system is that the pulp and catalyst do not need any tedious separation.

5. Study of adsorption of lignin derivatives on Pd/C catalyst (papers IV, V)

5.1. Background

The experiments in a flow-through reactor described above showed that the organosolv fractionation was a relatively fast process and that he transfer hydrogenolysis over Pd/C was slower. That is, although the organosolv pulping in the wood-containing cartridge was finished within 1 hour, the the hydrogenated products left the second cartridge only after 3 hours (Figure 13). The difference could arise due to the strong adsorption of lignin fragments on Pd/C. That suggested us the idea to study the interaction of lignin fragments with Pd/C separately.

5.2. Adsorption isotherms of lignin derivatives on Pd/C

First, to study the physical adsorption of lignin model species on Pd/C, we reproduced the molar ratio of water, methanol, palladium, and lignin which was characteristic of the flow reactor, $(4 \times 10^3) : (4 \times 10^3) : 1 : 2$, respectively. Concentrations of individual lignin species (**1−7**) were varied to obtain the dependence of adsorption on the concentration. Pd/C, solvent, and model compound were mixed in a test tube and vigorously stirred for 20 min. The mixture was then filtered and extracted, and the species which remained desorbed were quantified with NMR.

The results were processed using the Langmuir isotherm equation which binds the concentration of dissolved compound with the degree of adsorption.

$$a \left[\frac{\text{mmol compound}}{\text{gram Pd/C}} \right] = \frac{a_0 K c}{1 + K c} \qquad \text{(Eqn. 6)}$$

This is the simpliest model and it does not take into account the possibility of multilayer adsorption and the interactions of adsorbed molecules within the single layer. There are only two parameters; a_0 is the maximum surface coverage which is achieved in case of very high concentrations, and K is adsorption equilibrium constant:

$$K = \frac{\theta}{(1 - \theta)c} \qquad \text{(Eqn. 7)}$$

where $\theta = a/a_0$ is the surface occupation degree.

Advanced models implement more than two parameters and therefore require much higher accuracy of measurement. It is also more complicated to bind the variety of parameters with the features of molecular structure.

For each compound, a C code was used to find values a_0 and K, which correspond to the minimum standard deviation (σ_{min}) of the calculated adsorption versus experimental data. Ranges of values of a_0 and K were found in which $\sigma \leq 1.01\sigma_{min}$.

Dimeric compound **17** exhibited the highest affinity toward the catalyst surface (Figure 16 and Table 9), with adsorption constant $K = 7.0 \times 10^3$ L·mol^{-1}. Monomer **13** is formed as the main product of the first stage of solvolysis of hardwoods (i.e., birch). This compound also demonstrated a high adsorption constant $K = 6.6 \times 10^3$ L·mol^{-1}, which can be explained by the presence of electron-rich aryl, a double bond, and two hydroxyl groups that can bind to the catalyst surface. The two methoxy groups can also increase the coordination by donating electron density to the aryl.

Allylic alcohol **14** with guiacol unit demonstrated surprisingly low affinity toward the catalyst ($K = 1.5 \times 10^3$ L·mol^{-1}), presumably to the absence of the second methoxygroup and therefore too weak coordination of the aryl ring. 4-(3-hydroxypropyl)syringol **7**, a product of hydrogenation of monolignol **13**, had lower adsorption constant ($K = 3.4 \times 10^3$ L·mol^{-1}) than that of **13**, which suggests that the presence of the double bond is important for efficient bonding. For guaiacol derivative **3**, a significantly lower affinity was observed ($K = 0.3 \times 10^3$ L· mol^{-1}) compared with that of the syringol analogue. This supports the idea that methoxy groups coordinate relatively strongly to the palladium surface.

Propylphenols **6** and **2**, formed by complete hydrogenation of side chain in lignin fragments, were finally studied. Syringol propane **6** had, as expected, a further decrease in the adsorption ability ($K = 1.2 \times 10^3$ L·mol^{-1}) as compared to **7** ($K = 3.4 \times 10^3$ L· mol^{-1}) and **13** ($K = 6.6 \times 10^3$ L·mol^{-1}). In the case of guaiacol propane **2**, an unexpected increase was observed ($K = 1.7 \times 10^3$ L·mol^{-1}) as compared to **3** ($K = 0.4 \times 10^3$ L·mol^{-1}), and the adsorption was similar to that of substrate **14** ($K = 1.5 \times 10^3$ L·mol^{-1}).

According to these results, the species emerging during the initial solvolysis of lignocellulose tend to bond to Pd/C surface stronger than the final hydrogenation products, which can explain the difference of the apparent rates of solvolysis and hydrogenation.
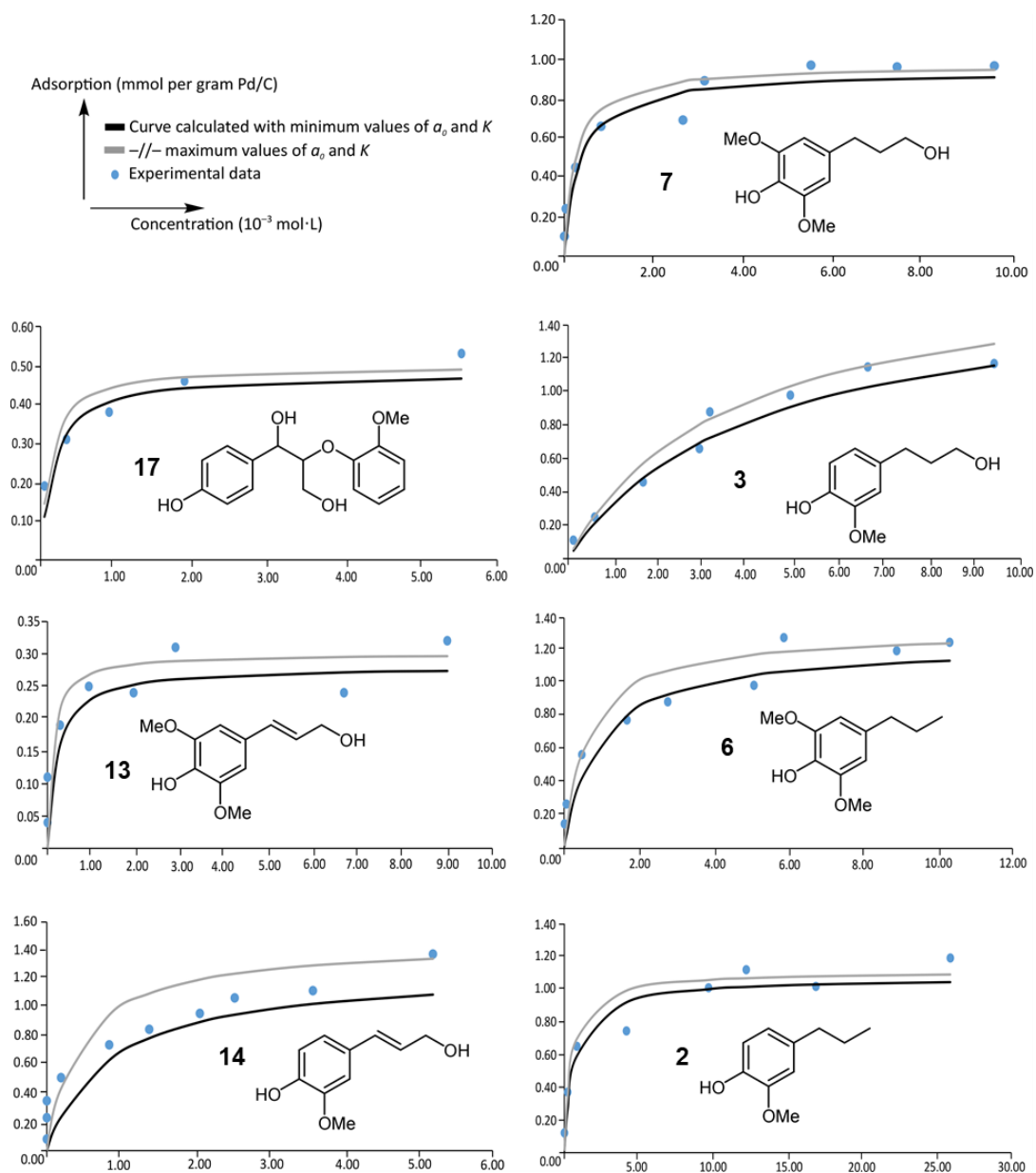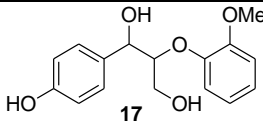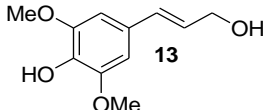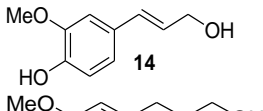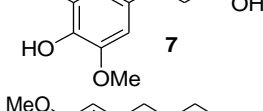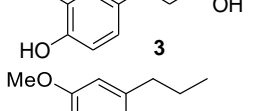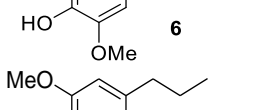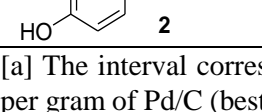
Figure 16. Adsorption curves of lignin model compounds on Pd/C.[iii]

Table 9. Parameters of the Langmuir isotherm for the studied lignin compounds

Structural formula	Max. adsorption a_0 [a][b]	Adsorption constant K [a][c]	σ_{min}
17	0.48–0.50 (0.49)	6.0–8.1 (7.0)	0.04
13	0.28–0.30 (0.29)	4.6–8.8 (6.6)	0.05
14	1.27–1.46 (1.37)	1.2–2.2 (1.5)	0.16
7	0.94–0.97 (0.95)	2.9–4.0 (3.4)	0.08
3	1.65–1.76 (1.70)	0.2–0.3 (0.3)	0.06
6	1.24–1.32 (1.31)	1.1–1.6 (1.2)	0.11
2	1.07–1.11 (1.09)	1.5–2.0 (1.7)	0.10

[a] The interval corresponding to $\sigma \leq 1.01\sigma_{min}$. [b] Mmol of substrate per gram of Pd/C (best-fitting value). [c] 10^3 L·mol^{-1} (best-fitting value).

A linear correlation ($r^2 = 0.89$) was observed between the maximum surface coverage a_0 and the free energy of adsorption expressed as $\Delta G_{ads} = -RT \ln K + \text{const}$. This trend (Figure 17) can be explained as follows. It is reasonable to assume that a_0 is in inverse ratio to the characteristic surface area occupied by a single molecule in the saturation state: $a_0 = u_1/s - u_2$, where u_1 and u_2 are parameters corresponding to the fact that a_0 becomes zero under finite values of s (it is not necessary to have infinite s to get $a_0 = 0$). u_1 is a proportionality coefficient which may be considered to be roughly equal to the overall active surface of the catalyst. The ratio u_1/u_2 has the physical sense of the maximum surface area of a molecule which still can be adsorbed. Therefore, $s = u_1/(a_0 + u_2)$. If the majority of the surface is occupied by solvent or if the bonding sites are represented by small nanoparticles, the bonding of very large molecules is impossible. Then $u_2 \gg a_0$ and $s \approx u_1(u_2 - a_0)/u_2^2$, i.e. s is tentatively a linear function of a_0. On the

other hand, s is aligned with what can be called effective number of sites by which the adsorbed molecule is bounded to the surface. Therefore s indeed may be linearly dependent on the free energy of bonding and so far as $s(a_0)$ is linear, $\Delta G(a_0)$ is also linear.
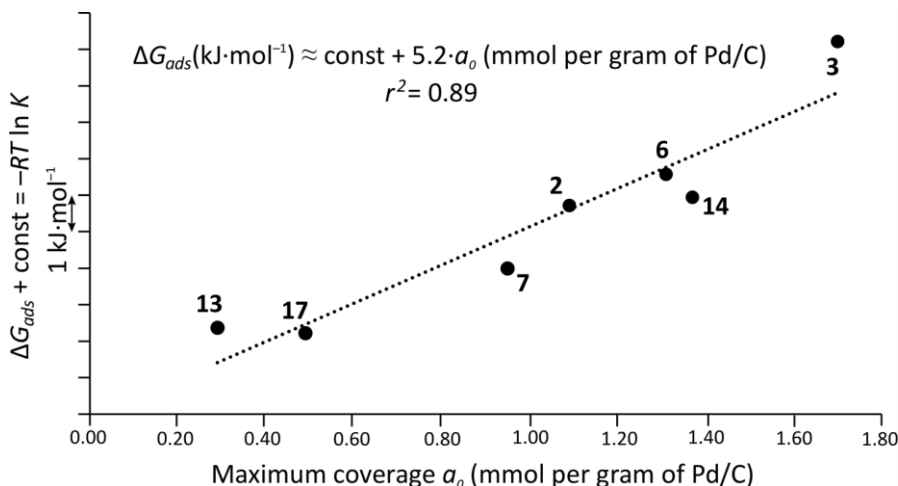

Figure 17. Linear correlation of maximum surface coverage a_0 with ΔG_{ads} $= -RT \ln K +$ const. Each point corresponds to the molecule with the specified number.

5.3. Theoretical study of lignin fragmentation over Pd catalyst

To get further insight into the mechanism of lignin transformation in the developed system, we have studied the interaction between model species and the Pd catalyst theoretically. We implemented the method of reactive force-field (ReaxFF) and quantum chemistry calculations [62] [63] [64] to model the conditions inside the Pd-containing cartridge of the flow-through system.

The ReaxFF method fills the gap between methods fully based on the principles of quantum chemistry, and methods implementing classical interatomic potential energies.[65] The first of the mentioned groups of methods consider electronic structure of molecules and even though it affords higher accuracy, the procedures are too computationally tedious to be used when dealing with large systems. The second group of methods, on the contrary, require much less computational resources and is preferred for simulations over longer time-scales and larger scales. However, the bonds between atoms are supposed to be predefined, therefore it is impossible to simulate chemical reactions in these cases. The ReaxFF method combines advantages of both approaches by introducing an empirical potential of interaction between atoms, thus avoiding extensive calculations through quantum mechanics.

The model species selected for this study, a dimer with β-O-4′ linkages (**18**) and an allylic monolignolic alcohol (**13**), are shown in Scheme 12. These species contain the structural motifs which have been experimentally shown to play the main role in the considered transformation. For the compound **18**, we focused on the Pd-catalyzed cleavage of C–O bond, and for **13** on the hydrogenation of the double bond.
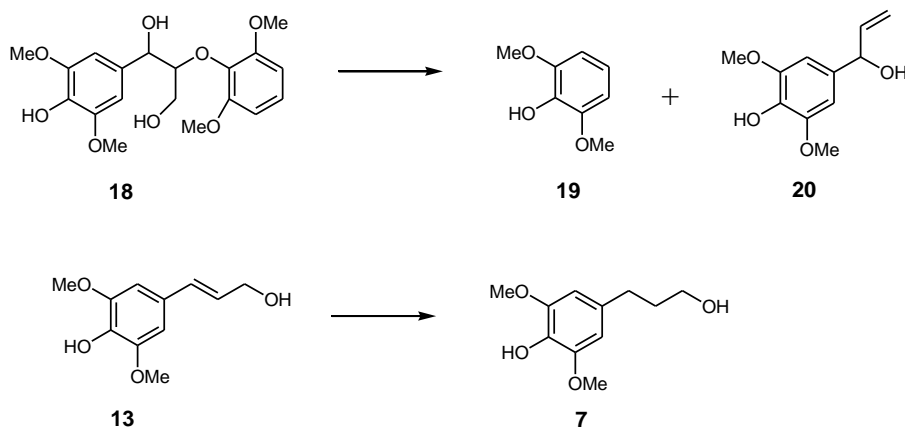
Scheme 12. The molecular species and fragmentation products observed in the simulation

Figure 18 displays the energy and structure of a system made up of Pd surface, **18** (β-O-4′ model) and the solvent as a function of the simulation time together with selected structures which represent various steps of the mechanism. Configurations A–C correspond to the initial adsorption of 18 on Pd surface, with gradual strengthening of the binding between the benzylic oxygen and the surface. In the configuration D, a chemical bond appears, with simultaneous cleavage of the O-H bond in the initial structure and also with binding of the H atom to the surface. The process of the chemical adsorption takes ∼10 ps and is followed by cleavage of the ether C-O bond. Syringol (**19**) is then readily desorbed from the surface while the other fragment (**20**) is still strongly bonded and can be hydrogenated further to afford the final products. Before separation, the two fragments **19** and **20** are oriented in parallel (Figure 18, I) due to π-stacking interaction between aromatic rings.
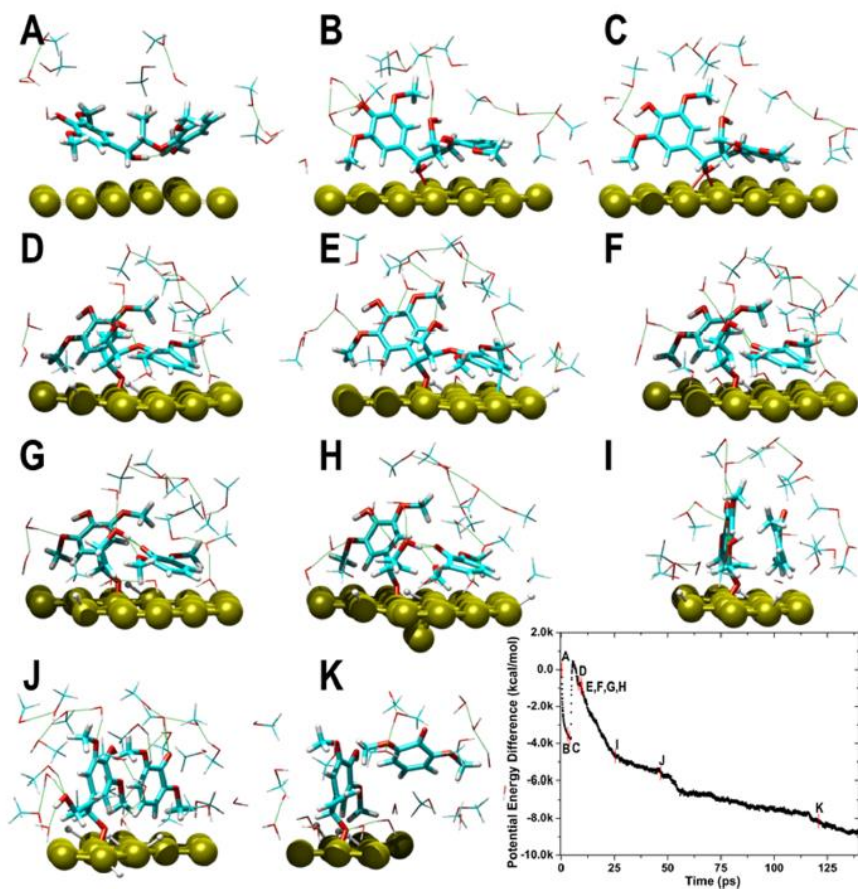
Figure 18. A–K, intermediate structures from the simulation of the adsorption of 18 on the Pd surface. Plot, evolution of the potential energy of the system with time.

In the case of molecule **13**, we studied hydrogenation of the double bond over the Pd surface. The process of hydrogenation starts with adsorption of aromatic ring. Figure 19 shows the gradual elongation of C–C distance as the result of double bond cleavage and binding of the carbon atoms to the surface. This is accompanied by formation of the new C–H bond. Rough estimates of the adsorption energies were obtained through a calculation taking into account only the interaction between the Pd surface and the adsorbed molecule, not including the surrounding species. The adsorption energy of the initial species (double bond) is −101 kcal/mol which is higher than of the final species (single bond + hydrogen) by ca. 50 kcal/mol. More accurate calculation gave results of –109 and −100 kcal/mol, respectively. Therefore, the hydrogenated products should have a relatively higher concentration in the solution. (These values should be considered limits of the real energies, as they still do not include all interactions which might weaken adsorption.)
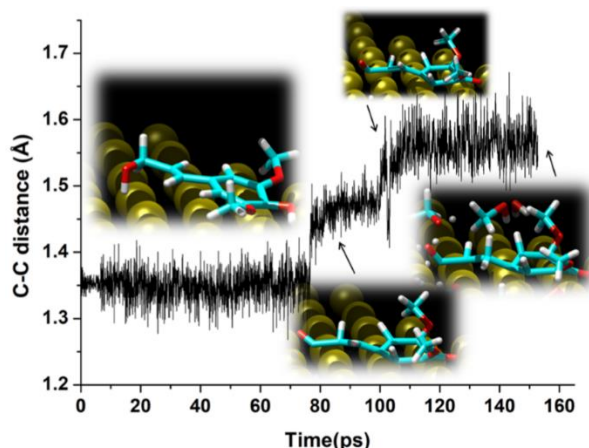
Figure 19. Elongation of the C−C bond in the **13** as the result of hydrogenation.

5.4. Summary

We have studied the adsorption isotherms of several lignin model molecules on the Pd/C catalyst. The results are in accordance with previous observations of the flowthrough system. The dimeric model compound, illustrating the native β-O-4′ bond, possesses the highest adsorption equilibrium constant (7.0×10^3 L·mol^{-1}). The monolignols that are also formed during organosolv pulping in the absence of catalyst demonstrate slightly lower but still significant values (6.6×10^3 and 1.5×10^3 L·mol^{-1}). The products of hydrogenation show smaller affinity toward the catalyst surface ($0.3-3.4 \times 10^3$ L·mol^{-1}). The maximum surface-coverage values correlate with the free energy of adsorption, which might mean that characteristic catalyst surface per adsorbed molecule.

Further computational studies revealed the mechanism of transformation of the adsorbed lignin species. For the β-O-4′ model molecule **18**, cleavage of the C-O bond was observed, and in case of monolignol with allyl moiety **13**, hydrogenation of the double bond. Both reactions led to the fragments which correspond to those obtained in the experiment.

6. Concluding remarks

The thesis describes research dedicated to valorization of various types of woody biomass; bark and heartwood of oak (*Quercus suber*) and birch (*Betula pendula*). Through these examples, we have demonstrated new approaches for processing of two components of the biomass: suberin polyester and lignin polyether.

In the case of bark, conventional lignin-first approach was not efficient as the suberin was not depolymerized and instead we ran the lignin-first under slightly basic conditions (NaOH). First, we applied a Pd-catalyzed process to *Quercus suber* bark. Suberin and lignin were depolymerized, and the product mixture consisted of monomers from both lignin and suberin as well as oligomers of both. By applying a three-step deoxygenative process, we could valorize both suberin and lignin into hydrocarbon bio-oil (42% of bark weight, 64% of total bark carbon), and obtain 4-ethylguaiacol (**1**) (2.6% bark weight, 90% purity) as the product of partial reductive depolymerization of lignin. The bio-oil have been extensively studied with GC-MS, 2D GC, and Simulated distillation techniques. It was shown to contain C_6–C_{27} hydrocarbons and has average molecular formula $C_{14.9}H_{28.4}O_{0.00-0.06}$, which leads to the estimated heat of combustion 46–49 MJ·kg^{-1}.

To overcome the drawbacks of the procedure with Pd catalysis such as pulp contamination with salt and metal, we developed a different method which implements a recyclable, salt and metal-free solvent system of MeOH–H_2O–Et_3N. Triethylamine plays the role of a basic catalyst for hydrolysis of ester bonds in the bark tissue. For hydrodeoxygenation, we treated the solubilized lignin and suberin with hydrogen gas in the presence of Pt catalyst. As the product, a fuel within the gasoline–aviation– diesel range was obtained with a 40% yield from the initial bark mass. At the industrial scale, the procedure is expected to become affordable, requiring only 23 MJ of energy to yield 1 kg of diesel product.

In the case of *Betula pendula* wood, we have developed a procedure for biomass fractionation under continuous flow conditions. The method affords metal-free cellulose pulp of high quality (87% enzymatically produced glucose yield) and lignin-derived aromatic monomers (39% NMR yield, 83% of theoretical maximum). The system implements internal hydrogen donors (hemicellulose, solvent) to accomplish the process of trapping the lignin intermediates. Both pulping of biomass and the reductive trapping of intermediates were for the first time accomplished separately in space and time within

one flow-through system. It was found that under the employed pulping conditions lignin is partially reductively cleaved into monolignols even in the absence of metal catalyst. These unstable allylic alcohols are trapped by the Pd/C catalyst which hydrogenates their double bonds and thus stabilizes them. The Pd/C is also responsible for depolymerization of oligomeric fragments of lignin, presumably by cleaving less available ether linkages. The yield of lignin monomers is 21% without catalyst and 39% with the catalyst (the latter corresponds to 83% of theoretical maximum estimated from β-O-4' bond content). The yield of enzymatically produced glucose is 87% of the cellulose content in the biomass.

The data obtained in the flow system were complemented with a study of adsorption isotherms of several lignin model molecules on the Pd/C catalyst. The results allowed to explain the difference in rates of processes of lignin solvolysis and consequent hydrogenolysis of the intermediates; the affinity of dimeric β-O-4' model and monolignols toward Pd/C surface is higher than that of saturated products. Further computational studies revealed the mechanism of transformation of the adsorbed lignin species. For the β-O-4′ model molecule **18**, cleavage of the C-O bond was observed, and in case of monolignol with allyl moiety **13**, hydrogenation of the double bond. Both reactions led to the fragments which correspond to those obtained in the experiment.

7. Acknowledgements

> Om kvällen skall dagen prisas.
> *Hávamál, 81*

I wish to thank those who helped me:

Prof. Joseph Samec for being a very patient supervisor, giving me enough freedom, and for all scientific and emotional support. It was a great luck for me to get into Joseph's group.

My co-supervisor **Prof. Göran Widmalm** for being very nice and also excellent teacher of the NMR course.

Prof. Pher Andersson for his interest in this thesis and helping with the draft.

Prof. Yuriy Roman of MIT for accepting me for exchange project in his group and helping me with valuable advices, and **Michael Stone** for his kind, but strict and efficient guidance throughout this time.

My collaborators: **Dr. Jonas Sävmarker, Prof. Mats Larhed, Dr. Susanna Monti, Dr. Pemikar Srifa, <u>Dr</u>. Elena Subbotina, Kranti Navare, Natalia Crespo Mendes, Dr. Vincent Placet, Dr. Karel Van Acker,** – we wouldn't have published these articles if we didn't work together.

Members of Joseph Samec group: **Dr. Rahul Watile, Dr. Sunisa Akkarasamiyo, Dr. Anon Bunrit, Dr. Jessica Margalef, Dr. Pemikar Srifa, Dr. Rabiya Ayub, Davide Di Francesco, Dr. Sari Rautiainen, Daria Lebedeva, Dr. Thanya Rukkijakan, Dr. Kuntawit Witthayolankowit, Withsakorn Sangsuwan, Suthawan Muangmeesri, Violetta Pospelova, Gonzalo Castiella, Alberto Alonso, Dr. Kiran Reddy**, for being nice labmates and colleagues.

Mikko, Cyril, Leif, Anton, and especially **Dr. Ning Li** for our interesting philosophical talks. Ning, I wish you a great success which you deserve for your hard work!

Dr. Daniels Posevins and **Igor Lebedev,** for being supportive at the time when I was writing the thesis.

Dr. Maxim Galkin for all his help, for our productive collaboration and discussions. If not Maxim, I probably wouldn't have finished my PhD!

Members of RenFuel company: **Dr. Alexander Orebom, Dr. Christian Dahlstrand, Dr. Johan Verendel, Dr. Marcus Ruda**, and especially **Dr. Joakim Löfstedt** for introducing me into Swedish cycling clubs and competitions.

My cycling companions in Uppsala: **Marko, Pär, Bella, David, Daniel**, **Sebastian**, and others.

Viktoria for taking the photo which I used as cover picture.

Maxim and **Ivan** for all great sporting time we had together.

Teachers of Moscow Chemical Liceum, Moscow State University, and RAS Higher Chemical College. I especially thank members of group of molecular spectroscopy of MSU for their enormous patience during my master's studies.

My family, – for we are the same that our fathers have been;
we see the same sights that our fathers have seen;
we drink the same stream, and we feel the same sun,
and we run the same course that our fathers have run.

Anders Tegnell and other Swedish authorities for protecting my freedom in summer 2020. I've been watching admiringly how you prevented the country from lockdown.

Sweden, for the boundless hospitality, and for these calm years. You are an island of peace and sanity in this crazy world. Tack, mitt älskade land!

8. Appendix

This section contains a more detailed description of 2D GC and Simulated distillation techniques.

6.2. Simulated distillation

Physical distillation of bulk samples is widely used to determine the boiling point ranges. Simulated distillation, first introduced in 1960,[66] is a gas chromatography technique which is an alternative to the physical distillation. The procedure requires only a microlitre sample and is rapid, reproducible, and easily automated, and is widely used to analyze hydrocarbon mixtures.

Simulated distillation algorithm implements the property of hydrocarbons to be eluted from a nonpolar column in boiling point order. The column temperature is tuned so that all sample is eluted. The retention times of the mixture components are correlated to temperature by running a standard mixture in the same conditions. The standard typically consists of a range of linear alkanes with known boiling points. Using the GC data, it is possible to build the distillation curve, i.e. to calculate the percentage recovered at any temperature.[67]

6.1. Two-dimensional gas chromatography (2D GC)

A 2D GC experiment implements combination of two chromatographic columns with different stationary phases. The output of the first column is a sample stream for the second one. The samples a taken regularly throughout the process and thus a secondary chromatogram is generated for each point of the primary chromatogram. All substances containing in the initial mixture pass through both columns. Each substance is characterized by two retention times, which are determined by the interaction of the substance with two independent stationary phases. The resulting plot is therefore a 2D chromatogram.[68] 2D GC is able to separate isomers of hydrocarbons. By running a sample and comparing the sample to a library of known standards, very detailed information of a sample is obtained. This methodology is used in the petroleum industry.
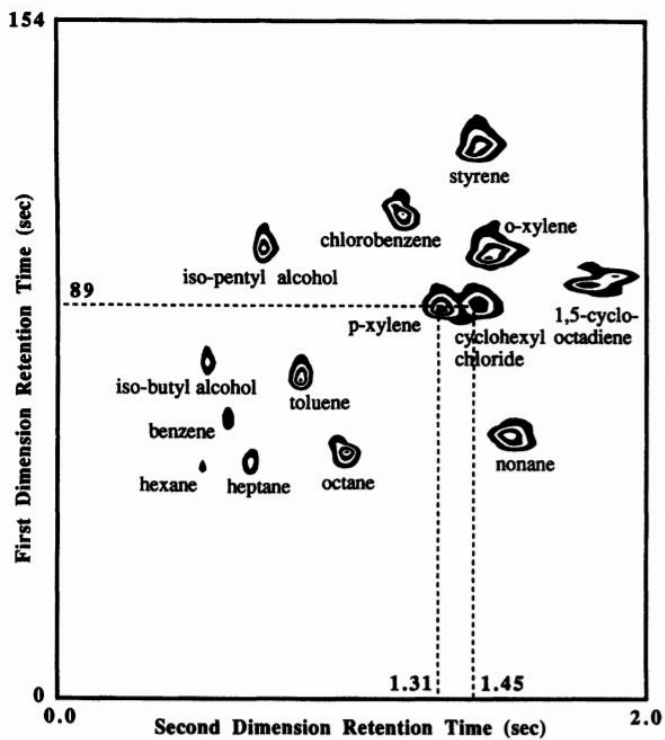
Figure 19. A typical 2D GC chromatoram.

9. References

[1] F. D. Pileidis and M.-M. Titirici, *ChemSusChem*, **2016**, *9*, 562.

[2] C. M. Welker, V. K. Balasubramanian, C. Petti, K. M. Rai, S. DeBolt and V. Mendu, *Energies,* **2015**, *8*, 7654.

[3] A. Sen, M. Zhianski, M. Glushkova, K. Petkova, J. Ferreira and H. Pereira, *Wood Sci. Technol.,* **2016**, *50*, 1261.

[4] U. Biermann, U. Bornscheuer, M. A. R. Meier, J. O. Metzger and H. J. Schäfer, *Angew. Chem. Int. Ed.*, **2011**, *50*, 3854.

[5] J. Ralph, *Phytochem. Rev.,* **2010**, *9*, 65.

[6] R. Vanholme, B. Demedts, K. Morreel, J. Ralph and W. Boerjan, *Plant Physiol.*, **2010**, *153*, 895.

[7] G. Henriksson, *Lignin, in Wood Chemistry and Wood Biotechnology Vol. 1* (Eds.: M. Ek, G. Gellerstedt, G. Henriksson), De Gruyter, Berlin, 2009, pp 121–144.

[8] H. Sixta, *Introduction, in Handbook of Pulp, Vol. 1* (Ed.: H. Sixta), Wiley-VCH Verlag GmbH, Weinheim, Germany, **2006**, pp 2–9.

[9] Y. Sun, J. Cheng, *Biores. Technol.,* **2002**, *83*, 1.

[10] J. C. Moura, C. A. Bonine, J. de Oliveira Fernandes Viana, M. C. Dornelas and P. Mazzafera, *J. Integr. Plant Biol.,* **2010**, *52*, 360.

[11] J. Graça, *Front. Chem.,* **2015**, *3*, 62.

[12] S. J. Vishwanath, C. Delude, F. Domergue and O. Rowland, *Plant Cell Rep.* **2015**, *34*, 573.

[13] A. Karnaouri, H. Lange, C. Crestini, U. Rova and P. Christakopoulos, *ACS Sustainable Chem. Eng.*, **2016**, *4*, 5289.

[14] A. Rossi, *Fuel Characteristics of Wood and Nonwood Biomass Fuels, in Progress in Biomass Conversion* (Eds.: D.A.Tillman, E.C.Jahn), Academic Press, **1984**, Chapter 2, pp 69−99.

[15] D. W. Goheen, *J. Chem. Ed.,* **1981**, *58*, 544.

[16] D. Peters in *White Biotechnology, Vol. 105* (Eds.: R. Ulber, D. Sell) Advances in Biochemical Engineering/Biotechnology (Ed.: T. Sheper), Springer-Verlag, Berlin, **2007**, p. 21.

[17] A. J. Ragauskas, C.K. Williams, B.H. Davison, G. Britovsek, J. Cairney, C.A. Eckert, W.J.Frederick, J.P. Hallett, D.J. Leak, C.L. Liotta, J.R. Mielenz, R. Murphy, R. Templer and T. Tschaplinski, *Science,* **2006**, *311*, 484.

[18] J. E. Holladay, J. F. White, J. J. Bozell and D. Johnson, *Top Value Added Chemicals from Biomass,* Pacific Northwest National Laboratory, Richland, WA, **2007** (report: PNNL-16983).

[19] Z. Strassberger, S. Tanase and G. Rothenberg, *RSC Adv.,* **2014**, *4*, 25310.

[20] G. Henriksson, J. Li, L. Zhang and M. E. Lindström, *Lignin Utilization in Thermochemical conversion of Biomass to Liquid Fuels and Chemicals, in RSC Energy and Environment Series, No. 1* (Ed.: M. Crocker), published by The Royal Society of Chemistry, Cambridge, UK, **2010**, pp 222.

[21] M. J. Climent, A. Corma and S. Iborra, *Green Chem.,* **2014**, *16*, 516.

[22] M. V. Galkin and J. S. M. Samec, *ChemSusChem*, **2016**, *9*, 1544.

[23] J. A. Geboers, S. Van de Vyver, R. Ooms, B. Op de Beeck, P. A. Jacobs and B. F. Sels, *Catal. Sci. Technol.*, **2011**, *1*, 714.

[24] A. Tejado, C. Peña, J. Labidi, J. M. Echeverria and I. Mondragon, *Biores. Technol.,* **2007**, *98*, 1655.

[25] W. Zhu, *Equilibrium of Lignin Precipitation – The Effects of pH, Temperature, Ion Strength and Wood Origins,* Thesis for the Degree of Licentiate of Engineering, Chalmers University of Technology, Gothenburg, Sweden, **2013**.

[26] W. G. Glasser, V. Dave and C. E. Frazier, *J. Wood Chem. Technol.,* **1993**, *13*, 545.

[27] T. M. Littiä, S. L. Maunu, B. Hortling, M. Toikka and I. Kilpeläinen, *J. Agric. Food Chem.,* **2003**, *51*, 2136.

[28] M. Funaoka, T. Kako and I. Abe, *Wood Sci. Technol.,* **1990**, *24*, 277.

[29] B. Saake, R. Lehnen, *Lignin, in Ullman's Encyclopedia of Industrial Chemistry,* John Wiley and Sons Inc., **2007**, 21, pp 21–35.

[30] S. Gillet, M. Aguedo, L. Petitjean, A. R. C. Morais, A. M. da Costa Lopes, R. M. Lukasik and P. T. Anastas, *Green Chem.,* **2017**, *19*, 4200.

[31] A. Vishtal and A. Kraslawski, *BioResources*, **2011**, *6*, 3547.

[32] E. Muurinen, *Organosolv Pulping. A Review and Distillation Study Related to Peroxyacid Pulping,* University of Oulu, Oulu, Finland, 2000, pp 13–75.

[33] P. Sannigrahi and A. J. Ragauskas, *Fundamentals of Biomass Pretreatment by Fractionation, in Aqueous Pretreatment of Plant Biomass for Biological and Chemical Conversion to Fuels and Chemicals* (Ed.: C. E. Wyman), John Wiley & Sons, Ltd, Chichester, UK, **2013**, pp 201–214.

[34] T. Renders, S. Van den Bosch, S.-F. Koelewijn, W. Schutyser and B. F. Sels, *Energy Environ. Sci.,* **2017**, *10*, 1551.

[35] X. Wang, R. Rinaldi, *ChemSusChem* **2012**, *5*, 1455.

[36] S. Van den Bosch, W. Schutyser, R. Vanholme, T. Driessen, S.-F. Koelewijn, T. Renders, B. De Meester, W. J. J. Huijgen, W. Dehaen, C. M. Courtin, B. Lagrain, W. Boerjan and B. F. Sels, *Energy Environ. Sci.,* **2015**, *8*, 1748.

[37] I. Klein, B. Saha and M. M. Abu-Omar, *Catal. Sci. Technol.,* **2015**, *5*, 3242.

[38] N. Yan, C. Zhao, P. J. Dyson, C. Wang, L. Liu and Y. Kou, *ChemSusChem*, **2008**, *7*, 626.

[39] M. V. Galkin and J. S. M. Samec, *ChemSusChem* **2016**, *9*, 1544.

[40] L. Shuai, M. T. Amiri, Y. M. Questell-Santiago, F. Héroguel, Y. Li, H. Kim, R. Meilan, C. Chapple, J. Ralph and J. S. Luterbacher, *Science,* **2016**, *354*, 329.

[41] T. Renders, W. Schutyser, S. Van den Bosch, S.-F. Koelewijn, T. Vangeel, C. M. Courtin, B. F. Sels, *ACS Catal.,* **2016**, *6*, 2055.

[42] M. D. Garrett, S. C. Bennett, C. Hardacre, R. Patrick and G. N. Sheldrake, *RSC Adv.*, **2013**, *3*, 21552.

[43] G. Koumba-Yoya and T. Stevanovic, *Catalysts,* **2017**, *7*, 294.

[44] G. Chatel, K. De Oliveira Vigier and F. Jérôme, *ChemSusChem*, **2014**, *7*, 2774.

[45] S.-F. Koelewijn, S. Van den Bosch, T. Renders, W. Schutyser, B. Lagrain, M. Smet, J. Thomas, W. Dehaen, P. Van Puyvelde, H. Witterse and B. F. Sels, *Green Chem.,* **2017**, *19*, 2561.

[46] D.Yu. Murzin, P. Mäki-Arvela, *Catalytic Deoxygenation of Fatty Acids and Their Derivatives for the Production of Renewable Diesel, in Thermochemical Conversion of Biomass to Liquid Fuels and Chemicals* (Ed.: M. Crocker); Royal Society of Chemistry, **2011**; Chapter 19, pp 496−510.

[47] W.F. Maier, W. Roth, I. Thies and P. V. Rague Schleyer, *Chem. Ber.*, **1982**, *115*, 808.

[48] N. Shinoda, E. Nagatomi, Lubricating composition for use in diesel engines compatible with biofuel, WO2009/013275 A1.

[49] A. Leung, D. G. B. Boocock and S. K. Konar, *Energy & Fuels,* **1995**, *9*, 913.

[50] E. Vonghia, D. G. B. Boocock, S. K. Konar and A. Leung, *Energy & Fuels*, **1995**, *9*, 1090.

[51] M. Snåre, I. Kubickova, P. Mäki-Arvela, K. Eränen and D. Yu. Murzin, *Ind. Eng. Chem. Res.,* **2006**, *45*, 5708.

[52] K. Kon, T. Toyao, W. Onodera, S. M. A. H. Siddiki and K. Shimizu, *ChemCatChem,* **2017**, *9*, 2822.

[53] A. Sen, M. Zhianski, M. Glushkova, K. Petkova, J. Ferreira and H. Pereira, *Wood Sci. Technol.,* **2016**, *50*, 1261.

[54] Q. Song, F. Wang, J. Cai, Y. Wang, J. Zhang, W. Yu and J. Xu, *Energy Environ. Sci*., **2013**, *6*, 994.

[55] A. X. Zeng, S.-T. Chin and P. J. Marriott, *J. Sep. Sci*. **2013**, *36*, 878.

[56] M. K. Jennerwein, M. S. Eschner, T. Wilharm, R. Zimmermann and T. M. Gröger, *Energy & Fuels,* **31**, *11*, 11651.

[57] D.W. van Krevelen, *Fuel*, **1950**, *29*, 269.

[58] J. Löfstedt, C. Dahlstrand, A. Orebom, G. Meuzelaar, S. Sawadjoon, M. V. Galkin, P. Agback, M. Wimby, E. Corresa, Y. Mathieu, L. Sauvanaud, S. Eriksson, A. Corma and J. S. Samec, *ChemSusChem*, **2016**, *9*, 1392.

[59] R. Järvinen, A. Silvestre, U. Holopainen, M. Kaimainen, A. Nyyssölä, A. M. Gil, N. C. Pascoal, P. Lehtinen, J. Buchert and H. Kallio, *J. Agric. Food Chem.,* **2007**, *55*, 1327.

[60] R. Järvinen , A. J. D. Silvestre , U. Holopainen , M. Kaimainen , A. Nyyssölä , A. M. Gil , C. P. Neto , P. Lehtinen , J. Buchert and H. Kallio, *J. Agric. Food Chem.,* **2009**, *57*, 9016.

[61] R. Itten, R. Frischknecht, M. Stucki, P. Scherrer and I. Psi, *Paul Scherrer Inst.,* **2014**, *June*, 1.

[62] S. Monti, V. Carravetta and H. Ågren, *J. Phys. Chem. Lett.* **2016**, *7*, 272.

[63] S. Monti, V. Carravetta and H. Ågren, *Small* **2016**, *12*, 6134.

[64] C. Zhu, S. Monti and A. P. Mathew, *ACS Nano* **2018**, *12*, 7028.

54

[65] T. P. Senftle, S. Hong, M. M. Islam, S. B. Kylasa, Y. Zheng, Y. K. Shin, C. Junkermeier, R. Engel-Herbert, M. J. Janik, H. M. Aktulga, T. Verstraelen, A. Grama and A. C. T. van Duin. *NPJ Comput. Mater.* **2016**, *2*, 15011.

[66] F.T. Eggerston, S. Groenings and J.J. Holst, *Anal. Chem.,* **1960**, *32*, 904.

[67] D.J.Abbott, *Journal of Chromatography Library,* **1995**, *56*, 41.

[68] Zaiyou Liu and John B. Phillips, *Journal of Chromatographic Science*, **1991**, *29*, 227.